LICENTIATE THESIS

Signal Processing and High Speed Imaging as Monitoring Tools for Pulsed Laser Welding

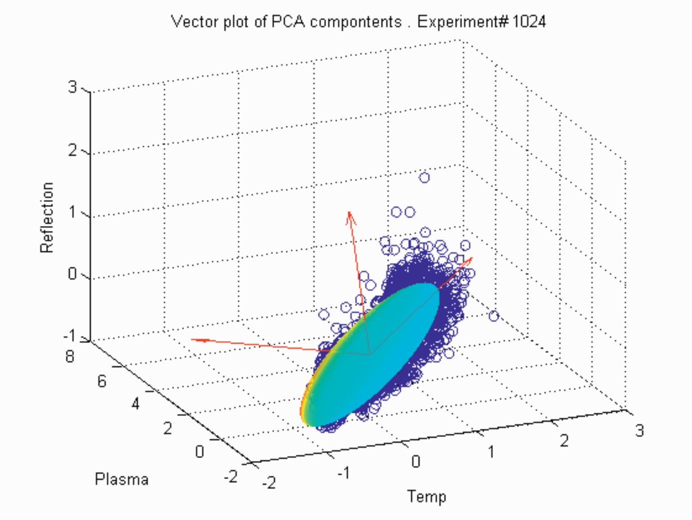

Rickard Olsson

LULEÅ
UNIVERSITY
OF TECHNOLOGY

Licentiate Thesis

Signal Processing and high speed imaging as monitoring tools for pulsed laser welding

Rickard Olsson

Division of Manufacturing Systems Engineering
Department of Applied Physics and Mechanical Engineering
Luleå University of Technology
Luleå, Sweden

in cooperation with
Laser Nova AB
Östersund, Sweden
Luleå, November 2009

Printed by Universitetstryckeriet, Luleå 2009

ISSN: 1402-1757
ISBN 978-91-7439-048-3

Luleå 2009

www.ltu.se

Dedicated to all the fools who never give up.

Preface

This research has been carried out at the Department of Applied Physics and Mechanical Engineering in the Division of Manufacturing Systems Engineering at Luleå University of Technology (LTU) and at Laser Nova AB in Östersund, Sweden.
I would like to express my gratitude to my supervisors Prof. Alexander Kaplan (LTU) and Prof. John Powell (LTU/Laser Expertise Ltd, Nottingham UK) for their guidance and support and good advice.

I am deeply indebted to my supervisor Prof. John Powell for bringing up good ideas, killing bad ideas and for his continuous pushing and for reviewing the papers in this thesis.
I am also grateful to my co author Ingemar Eriksson (LTU) for all the good discussions and the stimulating co-operation.

I would like to thank Prof. Fredrik Gustafsson at Linköping University for advice regarding statistical Signal Processing in general and Kalman Filtering in particular.
I would also like to thank Prof. em. Ingemar Ingemarsson at Linköping University for originally leading me into research studies and for introducing me into the beautiful field of Information Theory.

Finally I would like to thank my family and especially Maria for their encouragement and support during this long period.

Östersund, November 2009

Rickard Olsson

Acknowledgements

I am grateful to VINNOVA – The Swedish
Innovation Agency (project DATLAS, no. 2006-00668,
and Laser Nova AB Östersund, Sweden for their funding
and cooperation in the research.

Abstract

In Laser Materials Processing there has always been a need for suitable methods to supervise and monitor the processes on line, to ensure correct production quality or to trigger alarms when failures are detected. Numerous investigations have been made in this field, including experimental and theoretical work. It is common practice in this field to monitor surface temperature, plasma radiation and back-reflected laser light, coaxially with the laser beam. Traditionally, the monitoring systems involved carry out no statistical analysis of the signals received – they merely involve thresholds.

This thesis looks at the feedback collected during laser welding using such a co-axial setup from a Digital Signal Processing point of view and also uses high speed video photography to correlate signal perturbations with process anomalies.

.

Modern Digital Signal Processing techniques such as Kalman filtering, Principal Component Analysis and Cluster Analysis have been applied to the measurement data and have generated new ways to describe the weld behaviour using parameters such as reflected pulse shape. The limitations of commercially available welding supervision systems have been studied and design suggestions for the next generation of on line weld monitoring equipment have been formulated.

List of Publications

The licentiate thesis consists of four papers.

Paper I: State of the art of monitoring and imaging of laser welding defects,
R. Olsson, P. Norman, J. Powell and A. F. H. Kaplan
unpublished manuscript, 17 pages (Chapter 5 in the thesis)

Paper II: Advances in pulsed laser weld monitoring by the statistical analysis of reflected light.
R. Olsson, I. Eriksson, J. Powell and A.F.H. Kaplan
Submitted to J Phys D: Appl Phys, Oct 2009

Paper III: Challenges to the interpretation of the electromagnetic feedback from laser welding
R. Olsson, I. Eriksson, J. Powell, A. V. Langtry and A.F.H. Kaplan
Submitted to J Phys D: Appl Phys, Nov 2009

Paper IV: Ripple formation on the surface of laser spot welds.
I. Eriksson, R. Olsson, J. Powell, A. F. H. Kaplan and O. Sundelin
Submitted to J Laser Apps, Nov 2009

Additional relevant publication:
Pulsed laser weld quality monitoring by the statistical analysis of reflected light.
R. Olsson, I. Eriksson, J. Powell and A.F.H. Kaplan,
Proceedings of LIM 2009, Munich, June 15-19, 2009, WLT

TABLE OF CONTENTS

Preface……………………………………………………………I

Abstract…………………………………..…………………….III

List of Publications ……………………………………………….V

INTRODUCTION

1. Structure of the thesis……………….……………………….1
2. Motivation of the thesis ………………………………………1
3 Methodological approach ……………………………………..2
4. Introduction to laser welding, process monitoring and signal processing 4
4.1 Laser welding 4
4.2 Digital signal processing 6
4.3 Process monitoring …...7
5. State of the art 11
5.1 Introduction …..12
5.2. Results from literature and discussion 14
5.2.1 Microscopic post-process analysis of welding defects 14
5.2.2 Modelling and simulation of laser welding defects ……….15
5.2.3 High speed imaging of laser welding defects …................15
5.2.4 In-process monitoring of laser welding defects ....……17
5.3 Digital Signal processing 22
5.3.1 Time domain analysis 22
5.3.2 Frequency domain analysis …..24
5.3.3 CO2 welding using audible signals ……….........................24
5.3.4 Neural nets and fuzzy logic 23
5.3.5 Statistical signal processing methods 25
5.4 Conclusions 27
6. Summary of the papers 28
7. Conclusions 32
8. Future work 34
9 References ……………………………………………..…………33

ANNEX:

Paper I: (Paper I Corresponds to Section 5) 11
Paper II: Advances in pulsed laser weld monitoring by the statistical analysis of reflected light ……………………41
Paper III: Challenges to the Interpretation of the Electromagnetic Feedback from Laser Welding. ………………………63
Paper IV: Ripple formation on the surface of laser spot weld. 81

Introduction

1. Structure of the thesis

This thesis is composed of an introduction, a literature survey and three publications.

- Section 1 Describes the organization of the thesis.
- Section 2 The motivation behind the thesis
- Section 3 The methodological approach
- Section 4 A short summary of laser welding, process monitoring and signal processing.
- Section 5 State of the art.
- Section 6 Summary
- The publications

	Paper I	Paper II	Paper III	Paper IV
Sensors	●		●	
High speed imaging		●	●	●
CW welding			●	
Pulsed welding	●	●		●
On line analysis	●	●		
Off line analysis	●		●	●
Theory	●			

Table 1 Disposition of the four papers

2. Motivation of the Thesis

Lasers for Material Processing, especially Metal Processing have been in commercial use since the late 1970's and have today reached a high level of maturity and acceptance in fields ranging from heavy industry to aerospace, medical devices and basic research.

In industry, using lasers for welding purposes introduces a second challenge, namely the problem of how to ensure that the weld is free from defects by on-line

monitoring. This thesis deals with various approaches towards on-line monitoring and supervision of welding processes with a focus on pulsed Nd:YAG welding.
In all situations where laser light is absorbed by a metal it is transformed into heat. The way in which this happens, and how the metal absorbs or reflects the incoming light is one of the factors determining the weld quality and this is of primary interest for monitoring.
For supervision and monitoring two crucial questions are;

- What in the process can be measured?
- How accurately can we measure it and to what extent can we rely on, and draw conclusions from, these measurements?

Many of today’s commercial systems for weld supervision and fault detection are based upon the idea of a training phase where you tell the system what is a good weld and apply simple thresholds around a “golden template”. An alarm is triggered if the receives signal amplitude level goes outside the given limits.
This leads to a situation where much of the supervision is:

- Ad hoc. I.e. theoretical reasons for observed phenomena are not taken into account.
- Inflexible, and cannot systematically correlate the received signal, to failure reasons.

This thesis deals with various approaches towards on-line monitoring and supervision of welding processes with a focus on pulsed Nd:YAG welding.
In all situations where laser light is absorbed by a metal it is transformed into heat. The way in which this happens, and how the metal absorbs or reflects the incoming light is one of the factors determining the weld quality and this is of primary interest for monitoring.
For supervision and monitoring two crucial questions are;

- What in the process can be measured?
- How accurately can we measure it and to what extent can we rely on, and draw conclusions from, these measurements?

This research was carried out within the project DATLAS, which concentrates on the application of simple sensors to complex situation. This thesis therefore deals only with data collected from 1-dimensional sensors. I.e. no Digital Image Processing methods are included.

3 Methodological approach

The methodological approach of this Licentiate thesis can be understood by reference to the structure and order of the papers included. The work began with a literature survey of existing methods for welding supervision, covering sensor hardware, performance and detectable defects and what Digital Signal Processing (DSP) methods have been previously applied to measurement data for supervision and fault detection.

Paper I is a literature survey on the most common methods for laser welding supervision covering both defects, underlying phenomena, sensors and signal processing approaches.

Paper II presents two ways to detect abnormal weld pool behaviour.
In the first section of paper II DSP methods such as Kalman filtering, CUSUM detectors and Statistical Analysis was used to on one hand attenuate process and measurement noise and on the other hand to create ways to detect abnormal weld behaviour.
This statistical analysis was further expanded in section two of this paper where linear regression and clustering techniques were introduced as a way to track the weld behaviour all the way down to a single pulse.

Paper III presents a theoretical and experimental analysis of the practical limitations in a commercial supervision system. One main problem analyzed is the strong correlations between plasma and temperature signals found in the measurement data. A new way of presenting electromagnetic feedback from the weld zone – as a 3D data cloud is also presented in this work.
The ideas presented in paper III are straight-forward to implement in hardware or software.

Paper IV is a description of the resolidification of spot welded titanium observed from high speed imaging. This paper presents a qualitative explanation of the formation of surface ripples on the welds, together with results from high speed imaging, showing a method of reducing the ripple formation using suitable laser pulse modulation.,

4. Introduction to laser welding, process monitoring and signal processing

4.1 Laser welding

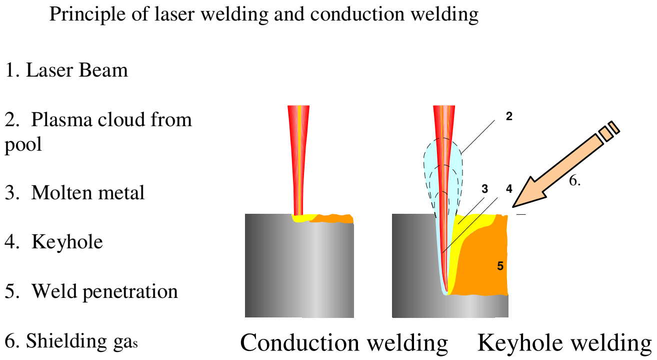
Principle of laser welding and conduction welding
1. Laser Beam
2. Plasma cloud from pool
3. Molten metal
4. Keyhole
5. Weld penetration
6. Shielding gas
2
3
4
5
6.
Conduction welding
Keyhole welding

Fig 1 Principle of laser welding

Laser welding is today a mature and widely used technique for joining materials together by using a focussed laser beam. The laser is focussed onto the substrate material as seen in Fig 1 creating a concentrated spot with a high power density - generating either a conduction weld or what is called a keyhole weld which penetrates deep into the material.

Lasers with power densities > 100 W/mm2 produce a keyholing action. The name “keyhole” originates from the fact that seen coaxially from above the combination of hole, melt front and rear area of resolidification forms a keyhole like shape. The keyhole is formed when a column of ionised metal vapour (Fig 1, (4)) forms below the beam impingement point, absorbing the incoming laser energy and converting it into heat generating the melt. The positive result of this is that narrow, deep welds can be achieved with small heat affected zones or alternatively, it is also possible to achieve very fast processing of thin sheets. This “keyhole” welding process is more efficient than a process where the weld shape is governed by thermal conduction only.

Advantages of laser welding

- Deep narrow welds
- Low heat affected zones (HAZ)
- Low distortion due to thermal impact

- High production rates
- Flexibility
- No tool wear
- Ease of automation

Laser Welding is used in

- Automotive industry, tailored blanks, car body, gear boxes etc.
- Shipbuilding industry
- Medical Devices, stainless, titanium
- Medical implants
- Micro mechanics

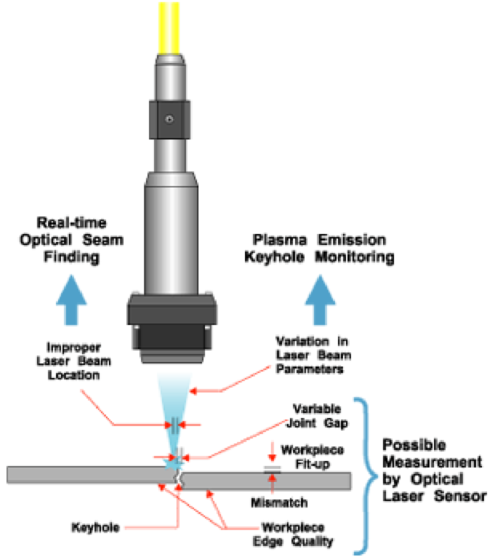
Real-time Optical Seam Finding
Plasma Emission Keyhole Monitoring
Improper Laser Beam Location
Variation in Laser Beam Parameters
Variable Joint Gap
Workpiece Fit-up
Possible Measurement by Optical Laser Sensor
Mismatch
Keyhole
Workpiece Edge Quality

Fig 2 Real world situation

The figure above shows a more detailed picture of a real world situation for the basic principle of laser welding .Here we can also see many of the common sources of defects, like misalignment, incorrect focus and non optimal gas flow,

4.2 Digital signal processing

Digital Signal Processing is a vast field that has had and has an enormous impact on research, industry and everyday life.
Digital Signal Processing or Signal Processing in short can be described in many different ways, one of which is here directly cited from Wikipedia:

> "*Signal processing is an area of electrical engineering and applied mathematics that deals with operations on or analysis of signals, in either discrete or continuous time to perform useful operations on those signals. Depending upon the application, a useful operation could be control, data compression, data transmission, denoising, prediction, filtering, smoothing, deblurring, tomographic reconstruction, identification, classification, or a variety of other operations.*
>
> *Signals of interest can include sound, images, time-varying measurement values and sensor data, for example biological data such as electrocardiograms, control system signals, telecommunication transmission signals such as radio signals, and many others.*"

Examples of tools used as Digital Signal Processing algorithms are,

- Fast Fourier transforms (FFT)
- Finite impulse response (FIR) filters
- Infinite impulse response (IIR) filters
- Wiener filters
- Kalman filters
- Echo Cancelling
- Beam forming.
- Adaptive filters

Signal Processing can then be further sub divided into categories like Audio-, Speech-, Image-, Video-, Array or Statistical Processing.

Statistical signal processing in particular is an area of Signal Processing where signals are treated as being observations from an underlying stochastic process. The processing deals with the statistical properties of the signals (observations) such as mean, covariance, etc...
In many areas signals are modelled as a sum $y(t)$ of a deterministic part $x(t)$ and a stochastic component $w(t)$. I.e.:

$$y(t) = x(t) + w(t),$$

where the noise part $w(t)$ is having a certain distribution such as Gaussian, flat, exponential, Rayleigh etc.

4.3 Process monitoring

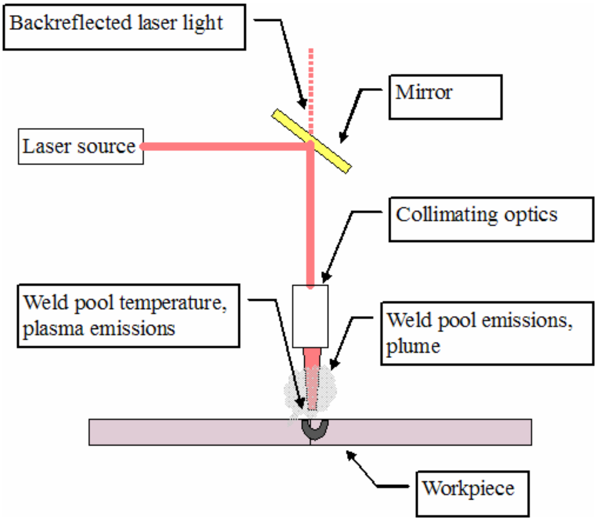
Backreflected laser light
Mirror
Laser source
Collimating optics
Weld pool temperature, plasma emissions
Weld pool emissions, plume
Workpiece

Fig 3 Monitoring setup

The monitoring situation in this work can typically be depicted as in the figure above. In this work we have limited ourselves to the analysis of:

- Weld pool infrared emissions.
- Plasma optical emissions
- Reflected laser light

These features were stipulated in the goal of the funding project DATLAS - to investigate the feasibility of using simple 1-D semi conductor sensors as a complement, and in certain situations an alternative, to more expensive and computationally intensive 2D-camera solutions.

Laser welding monitoring can roughly be divided into three different types:

- *pre-process*, arranged ahead of the welding zone like seam tracking devices for identifying the edge position;
- *in-process* monitoring, by on-line sensors observing the laser welding process. This can be done by using different sensors like photodiodes, cameras, pyrometers or acoustical sensors;
- *post-process* inspection is carried out after the weld has solidified, either during the welding process with camera sensors, or afterwards by visual inspection, x-ray, ultrasound, fluorescence, microscopy or other inspection or testing methods.

Classification of welding defects

Some common and important welding defects and their physical origin are summarised in **Table. 2.**

Defect	***Explanation of the physical cause***
Pore Void	Spherical gas bubble trapped by solidifying material Sharp edged volume caused by impurities or during resolidification
Blow-out	Caused by a near surface pore that opens and forms a crater
Crack H/C	Hot cracks are formed during solidifying in welded zone Cold cracks can form after welding, often in HAZ
Undercut	Not enough material in upper weld zone, depends on speed, power and gap
Root dropout	Too much molten material in lower weld zone
Penetration	Joint not completely penetrated, depends on oxidation, gas protection, contamination of gas or fluctuation of laser power
Lack of fusion	The laser misses the joint, partially or fully
Reinforcement	Too much material in upper weld zone, fluctuation of gap width

Table2: *Classification of laser welding defects and explanation of their physical cause*

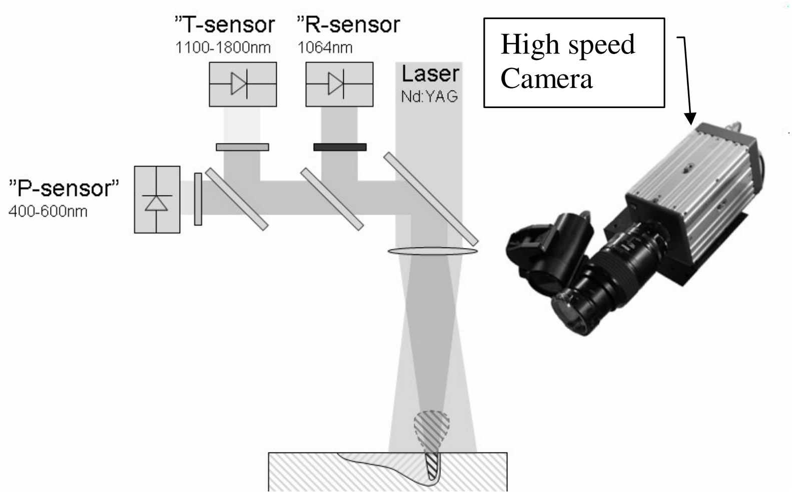

Fig. 4 *Typical setup*

The experiments involving pulsed welding were carried out using the set-up shown in **Fig. 4** above.

The use of 2D-sensors like cameras is an obvious and straight forward way of monitoring laser welding. There are however, a few drawbacks concerning cameras and Digital Image Processing techniques. One such drawback is the need for a high processing speed because the welding process involves dynamic processes in the ~10-20 kHz range. An on line monitoring system therefore requires frame rates in the order of several thousand frames per second. Such high frame rates lead to data transfer rates of several Gb/s and to be able to process data in real time this would often require dedicated hardware.

This need for high frame rates also introduces an illumination problem, because a high light intensity is needed to get clear images. Both these drawbacks lead to costly and technically sophisticated solutions which are inappropriate to smaller companies or low volume production.

One of the aims of this research was to see how much information about the welding process can be gathered using a simpler setup with only three 1D silicon photo diode sensors. High speed imaging was then used to correlate this data with the observed weld behaviour.

A commercial supervision system, having three sensors was therefore used: one sensor for surface temperature (T) measuring radiation in the $\lambda \in [1100 - 1800]\text{nm}$ interval, one for plasma radiation (P) ($\lambda < 600$ nm) and one for reflected laser light (R) centred around the Nd:YAG laser wavelength of1064 nm.

Data from the sensors were sampled at frequencies of; 8 kHz (paper II and III) and 20 kHz (paper 4).

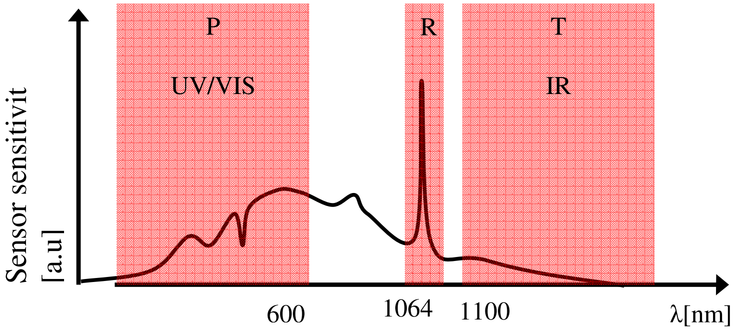

Fig 5 *Sensor sensitivity*

5. State-of-the-Art

Paper I.

State of the art of monitoring and imaging of laser welding

R. Olsson[1,2], P. Norman[1], H. Engström[1], A. F. H. Kaplan[1]

[1]Luleå University of Technology, Luleå, Sweden
[2]Laser Nova AB, Östersund, Sweden

Abstract

Several weld defects such as lack of fusion, blow-out holes, porosity, cracks and undercut can occur during laser welding. These defects can be crucial for product failure. Due to its complexity, the laser welding process and the origin of its defects are only partially understood. Both experimental observation and numerical simulation is difficult. Generally accepted knowledge of welding defects together with high speed imaging, X-ray transmission, and mathematical modelling have generated some understanding. However, experimental observation suffers from problems such as the small size of the process zone, its highly dynamic nature and the hot environment. In addition, the physical process is too complex for complete simulations.

As well as avoiding welding defects through process understanding, detection is of importance in industrial production. Monitoring can be divided into pre-, in- and post-process inspection, and between on- and off-line. Off-line post inspection is often expensive. Nowadays in-process monitoring is provided by photodiodes or cameras, but owing to the lack of fundamental process understanding, it is limited to empirical correlations between the appearance of a defect and signal changes.

The present review provides a survey on laser welding defects, on their experimental observation, on their theoretical treatment by modelling or simulation and on their detection by process monitoring. Despite wide ranging research efforts, the understanding and detection of laser welding defects is still very limited and unsatisfactory, and this hinders industrial implementation. Further research will be needed to fully control this critical welding process and in turn to guarantee reliable production and safe product function.

This survey is also considers methods for laser welding supervision from a Digital Signal Processing point of view. Both traditional 1-dimensional time or frequency domain methods as well more recent statistical and neural net approaches are covered.

Keywords: laser, welding, monitoring, imaging, defects, Digital Signal Processing

5.1 Introduction

The present paper provides a survey of literature on laser welding defects, divided into;

- microscopic post-process analysis of defects,
- mathematical modelling or numerical simulation of defect mechanisms,
- high speed imaging of the welding process and
- in-process monitoring of defects – which is the main focus of this work.

The motivation of this literature study is the research project DATLAS - which aims at improving commercial process monitoring systems (photodiode based) through an improved knowledge of the mechanisms causing the welding defects and monitoring signal changes. To succeed with this we have, together with eight companies, performed tests on different materials, joints and material thicknesses to accomplish a matrix correlating the weld defects to the sensor signal for these different setups. However, beside revealing empirical correlation rules, high speed imaging, in cooperation with simulation of radiation emissions impinging on the sensor, is planned in order to try to predict and explain the context between the physical mechanism of the dynamic welding process (in particular the defect origins) and dynamic signal changes. The main objective is to improve the capabilities and limitations of the defect-signal and of the signal interpretation.

Fig. 1 illustrates the connection between the laser welding process defects and how they can be monitored. The laser technique bubble in Fig. 1 includes; cw/pw, keyhole/conduction and laser/hybrid type welding

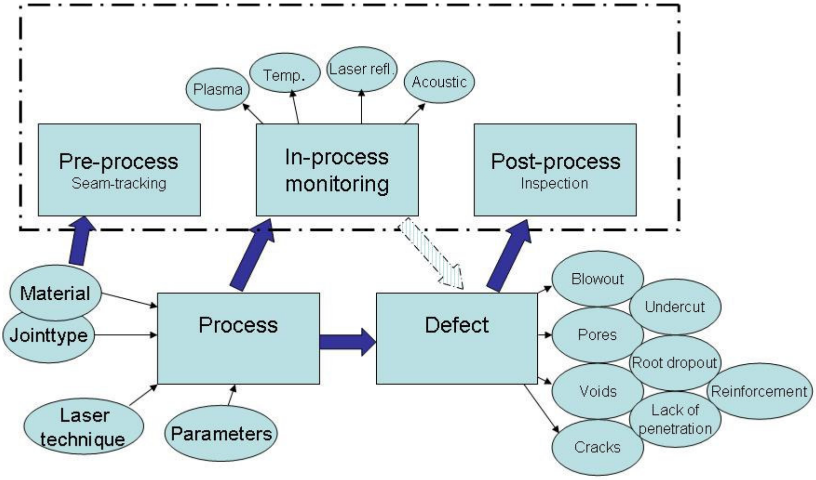
Plasma
Temp.
Laser refl.
Acoustic
Pre-process
Seam-tracking
In-process monitoring
Post-process
Inspection
Material
Jointtype
Process
Defect
Laser technique
Parameters
Blowout
Undercut
Pores
Root dropout
Voids
Reinforcement
Lack of penetration
Cracks

Fig. 1: Process-defect correlations and a classification of process monitoring/inspection methods

The monitoring can be divided into three different types:

(i) *pre-process*, arranged ahead of the welding zone like seam tracking devices for identifying the edge position;
(ii) *in-process* monitoring, by on-line sensors observing the laser welding process. This can be done by using different sensors like photodiodes, cameras, pyrometers or acoustical sensors;
(iii) *post-process* inspection is done after the weld has solidified, either during the welding process - with camera sensors or later - by visual inspection, microscopy or other inspection or testing methods.

Classification of welding defects

Some important welding defects [1] and their physical origin are summarised in **Tab. 1.**

Table 1: *Classification of laser welding defects and explanation of their physical cause*

Defect	***Explanation of the physical cause***
Pore Void	Spherical gas bubble trapped by solidifying material Sharp edged volume caused by impurities or during resolidification
Blow-out	Caused by a near surface pore that opens and forms a crater
Crack H/C	Hot cracks are formed during solidifying in welded zone Cold cracks can form after welding, often in HAZ
Undercut	Not enough material in upper weld zone, depends on speed, power and gap
Root dropout	Too much molten material in lower weld zone
Penetration	Joint not completely penetrated, depends on oxidation, gas protection, contamination of gas or fluctuation of laser power
Lack of fusion	The laser misses the joint, partially or fully
Reinforcement	Too much material in upper weld zone, fluctuation of gap width

These defects have been under serious investigation because they cause considerable problems to companies. The weld has to achieve appropriate mechanical properties under load conditions in order to maintain the function of the product. Weld failures weaken the material locally and can lead to fracture and catastrophic product failure. Therefore standardisation of welds and weld defects is essential, as well as their detection. All of the above defects have a three dimensional geometry and are therefore visible by the use of either ultrasound testing, X-ray or by observation of a cross section of the work-piece.

Process monitoring can support the detection of defect welds. However as it lacks 100% reliability, such detection is only indicative. Some of the defects are easy to detect on-line during the process, but others are very difficult. A single reliable sensor would be the most robust setup for the industry, as simple but reliable systems are wanted.

5.2. Results from literature and discussion

This section reviews the state-of-art of microscopic post-process analysis, mathematical modelling, process observation and process monitoring of welding defects.

5.2.1 Microscopic post-process analysis of welding defects

To be able to make accurate estimations of the type and level of defects occurring during welding, several specimens have to be evaluated. This is done either done by destructive mechanical testing (tensile testing, impact testing, fatigue testing, etc.), by destructive microscopic examination, or by non-destructive testing using ultrasound or X-ray methods to look inside the joint. A typical laser weld surface is shown in **Fig. 2(a)**. **Fig. 2(b)** shows a good weld after it has been polished and etched. **Fig. 2(c), (d)** shows a hot crack that has formed during resolidification of the weld. This type of crack can severely reduce the strength of the joint.

Welding defects can become the origin for fracture. Under certain load conditions plastic deformation takes place, along with the development of a stress field. Sharp corners or edges and constraints can act as stress raisers where very high stresses occur locally. This can initiate crack formation at the microstructural level, e.g. between grains. From these micro-defects crack propagation takes place. If the stress cannot locally relax sufficiently quickly, the fracture will propagate through the weld and result in failure. Product design is usually based on defect free welds of certain shapes and throat depths. The detection of welding defects is therefore essential, as it is a main cause for product failure.

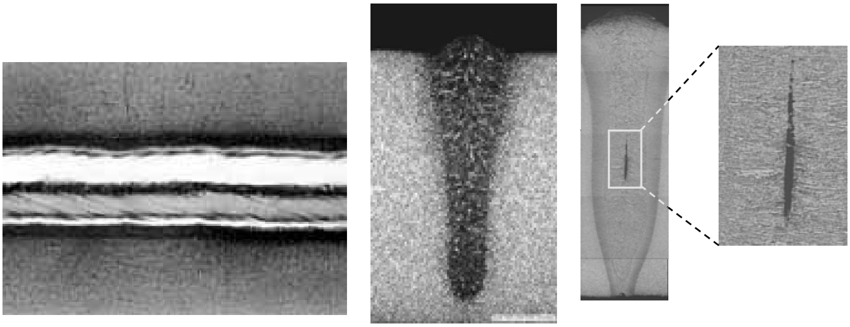

*Fig. 2: **(a)** weld surface, **(b)** cross section for a good joint, **(c)**,**(d)** hot crack*

5.2.2 Modelling and simulation of laser welding defects

Mathematical modelling and simulation can raise our understanding of the physical welding process. The development of a model can be supported by experimental observation, from which theories can be developed. Matsunawa and Katayama [2] have developed an X-ray imaging system together with a high speed camera to visualize the plasma and melt pool. With these tools they have explained how some aspects of the liquid motion in the melt pool and the plasma affect the welding result, e.g. pore formation.

The laser welding process is too complex to be fully simulated, but successful results in simulating parts of the process have been achieved by such researchers as Amara [3]. This work involved modelling the keyhole and melt pool movement that is affected by the flow of metal vapour in Nd:YAG laser welding. Fabbro [4,5] has also simulated the movement of the melt pool, metal vapour plume and keyhole during Nd:YAG laser welding. This work is also supported by high speed imaging of the weld pool motions. The work presents explanations of the keyhole behaviour and how the melt pool and vapour are coupled. Jin [6] modelled the keyhole in 3D by taking pictures of the keyhole during welding in glass and used this data to build the model. Thus it is clear that progress has been made, but there is still no complete prediction or description of the laser welding process, particularly in the context of welding defects. A keyhole model with melt flow and droplet ejection calculations [3] is shown in **Fig. 3**.

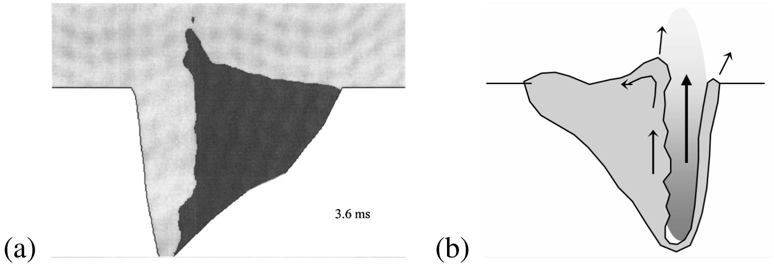

Fig. 3: (a) Simulation of the keyhole and melt pool flow, (b) explaining droplet ejection [3]

A model for explaining pore formation during the keyhole collapse after the end of a laser pulse [7] is shown in **Fig. 4**, explaining that recondensation of the metal vapour after pulse termination sucks the surrounding Ar-shielding gas into the keyhole which then collapses to include a cavity. During contraction the cavity becomes a stable spherical bubble where the surface tension pressure is in balance with the trapped Ar gas volume. During resolidification the slowly rising bubble becomes frozen into the weld as a pore.

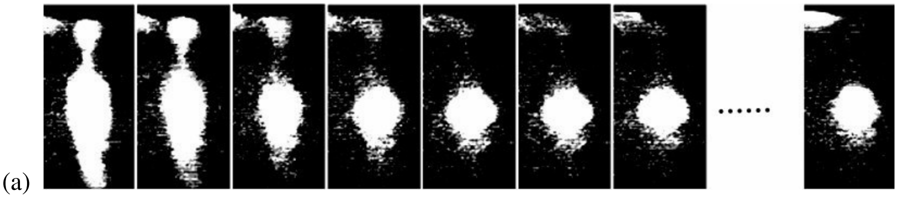

(b),(c)

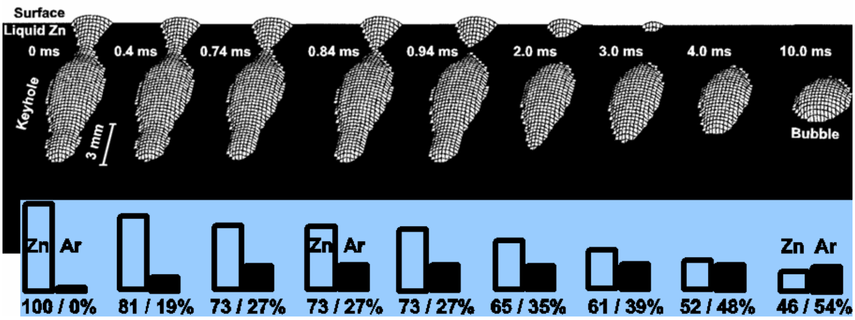

Fig. 4: *Keyhole collapse creates a bubble after termination of a laser pulse:* ***(a)*** *time sequence of X-ray images of the keyhole (side view),* ***(b)*** *contraction predicted by the model,* ***(c)*** *calculated mixture of metal vapour (Zn) and shielding gas (Ar) in the keyhole/cavity [7]*

Further models enable us to calculate the metallurgical composition in the laser weld cross section, for example - the amount of martensite formation leading to hot cracking susceptibility for a particular stainless steel [8]. For calculating the local fraction of martensite formed, several authors developed dendritic microstructure diffusion models. J. F. Gould [9] thermodynamically determined the critical cooling rate of martensite for Advanced High Strength Steel (AHSS) using sophisticated multi-scale modelling, e.g. at the grain size scale in conjunction with the macro-continuum scale. Also, the crack formation and propagation during load has been modelled to some extent [10],[11].

5.2.3 High speed imaging of laser welding defects

For observing the process in the simplest way a standard video camera can be used. However this has a very limited spatial resolution, giving poor image quality, and a limited frame rate and exposure time. This has the consequence that it will not be possible to accurately reproduce an image of laser welding. Several companies [12-15] have therefore developed different cameras that can observe the process. The cameras range from being able to reproduce an area of 1280x1024 pixels from 600 to 5000 frames per second. With lower resolution the frame rate can be as high as 30000. The price of the equipment is also determined by the dynamic range of the camera, which ranges from 8bit to 12bit from these companies. Today (2009) the price range is from 25000 USD to 90000 USD.

To observe the melt pool and keyhole clearly, a high brightness illumination is required whilst, at the same time, filtering out the broad bright spectrum brightness of the weld zone, particularly that of the plasma plume above the keyhole. Such filtering also succeeds for hybrid (laser+arc) welding [16], where the even stronger plasma radiation disturbs the observation. Such illumination can be achieved by either using spectrally narrow lamps, or a laser. As the laser gives a well defined wavelength it is simple to use with filters to get a good image quality, although it is possible to achieve very good quality using halogen lamps - as was done by Fabbro et al [4], where they look at stabilizing the melt pool with a gas jet, as shown in **Fig. 5(a),(b).**

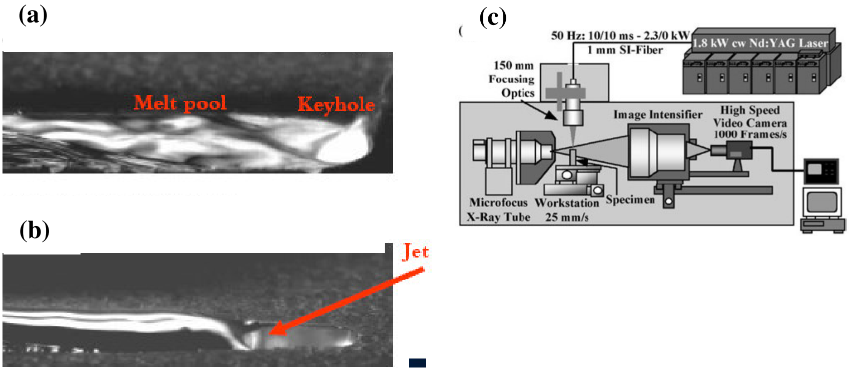
(a)
Melt pool
Keyhole
(b)
Jet
(c)
50 Hz: 10/10 ms - 2.3/0 kW
1 mm SI-Fiber
1.8 kW cw Nd:YAG Laser
150 mm Focusing Optics
Image Intensifier
High Speed Video Camera 1000 Frames/s
Microfocus X-Ray Tube
Workstation 25 mm/s
Specimen

***Figure 5**: High speed imaging of the top side of the melt pool and keyhole [4]: **(a)** weld pool waves, **(b)** calmed weld through an additional gas jet directed to the keyhole rear side. **(c)**Example of a set-up for X-ray high speed imaging [7]*

As shown in **Fig. 4(a)**, X-ray illumination of the weld zone from the side enables high speed imaging of the keyhole and pore formation. A typical experimental set-up [7] is shown in **Fig. 5(c)**. By the addition of tracer particles, e.g. carbides with high melting point, a contrast can be achieved that permits X-ray tracing of the particle trajectories corresponding to the flow inside the melt pool. Tin, having a low melting point, quickly dissolves in the weld pool and gives a contrast on the vertical weld pool shape during X-ray high speed imaging [2].

5.2.4 In-process monitoring of laser welding defects

Several monitoring techniques can be applied to laser welding, as shown in **Fig. 1.** In our research work we use in-process monitoring. This method of monitoring is used by several researchers because it gives most information about the process in a robust, simple manner when looking for defects, thus it also has high industrial potential.

State-of-the-art of monitoring

Table. 2 provides a survey of publications on in-process process monitoring of laser welding.

***Table 2:** Survey on publications on in-process monitoring*

No.	Author	Country	Laser system	Technoque	Power	Material	Thickness	Joint type	Defect	Inspection type	Monitoring sensor	Control loop
			CO2/ Nd-YAG	cw/ pw	kW		mm					
17	C. Bagger	DK	1	3	1,5	5	,5 1,25 2 3	13	25	27	31	+
18	A. Ghasempoor	Can	1	3	8	6	5	11	17,18,20,24	27	31-34	
19	H. K. Tönshoff	D	1, 16	3	6	6	10	12	20, 25	27	29-30	
20	H.B. Chen	UK	1	3	2 5	6	0,6 1 6	11	25	27	30	
21	A. Sun	US	1	3	1,1 7,4	6	0,91 1,2	13	25	27	30, 34	
22	Y. Kawahito	Jpn	2	4	0,05	5	0,1 1	15	24		29,31-32	+
23	B.N. Bad'yanov	Rus	2		1,4	6	0,5	13	25	27	29-32	
24	P.G. Sanders	US	1, 2	3, 4	6 1,6	5,6		14		27	30-31	
25	K. Kamimuki	Jpn	2		6	6,7	10	14	20,21,22,25	27	31	
26	K. Kamimuki	Jpn	2		3,5	6	6 10	11, 14	18, 20, 25	27	32, 34	
27	D. Travis	UK	2, 16		3	6		14			31, 33	
28	S. Postma	Ned	2		2	6	0,7	11	25		30-31	+
29	J. Petereit	D	1, 2						25	26-28	29-31	
30	M. Kogel-Hollacher	D						11		26-28	29	
31	J. Beersiek	D	1, 2									
32	F. Bardin	UK	2		4 2,5	8, 10		14	25	27	29, 31	+
33	M. Doubenskaia	F	2	3, 4	2					27	31	
34	M. Doubenskaia	F	2	4	3	6,7				27	31	
35	M. Doubenskaia	F	2	3	2	9	0,7 1	13	24	27	31	
36	Ph. Bertrand	F	2	3	3	6,7		11		27	31	
37	V.M. Weerasinghe	UK	1	3	2	6		11		27	30,32,34	
38	H. Gu	Can	1		1,7	6	1	11, 13	25	27	34	
39	D.P. Hand	UK	2	3	2	6	1	11, 13	25	27	30	+
40	S.-H. Baik	Kor	2	4	1	6	1	11		27	31	
41	L. Li	UK	1		2	6	5			27	34	
42	L. Li	UK	1	3, 4	1,5 5	5,6,8,9	2 0,22 1,5	11,13,15	25	27	30	
43	B. Kessler	D	1, 2	3					17,19,24,25	26-28	29-33	+
44	W. Wiesemann	D	1, 2							26-28		+
45	J. Shao	UK	1, 2						17, 19, 25	26-28	29-34	

TABLE LEGEND

Laser type	**Material**	**Joint**	**Defect**	**Inspection type**	**Sensor**
1=CO_2	5= Al-alloy	11=Butt joint	17=Blow-out 26=Pre-Process	29=CMOS-Camera	
2=Nd:YAG	6= Low C-steel	12=T-Joint	18=Void	27=In-Process	30=Plasma/ph.diode
3=Continous wave (cw)	7= Stainless steel	13=Lap Joint	19=Crack Hot/C.	28=Post-Process	31=T / photodiode
4=Pulsed wave (pw)	8= Titanium alloy	14=Bead on plate	20=Pores		32=Laser reflect./p.d.
16=Hybrid welding (MIG)	9= Zn-coated steel	15=Spot weld	21=Undercut		33=Voltage / current
	10=Inconel		22=Reinforcement	34=Acoustic / mic.	
			23=Root drop-out		
			24=Lack of fusion		
			25=Lack of penetration		

Scope of published experiments

The experiments in **Tab. 2** involve both CO_2 and Nd:YAG lasers in cw (continuous wave) and pw (pulsed) modes. Materials include mild and standard steel and different alloys such as Inconel, aluminium alloys and zinc coated steel. The thicknesses of these materials vary from 0,1mm to 10mm. Also the joint types are different, including Butt-, T- and Lap-joints, simplified Bead on plate welds and spot welding. All the defects shown in **Tab. 1** were monitored with on-line sensors such as cameras, photodiodes and acoustic emission sensors.

Monitoring techniques

Photodiode sensor: To be able to observe a process, a sensor is needed. For laser welding is a high temperature process with accompanying thermal emissions so optical sensors are favoured, in contrast to e.g. machining, which is a vibration governed process where acoustic and vibration sensors are preferred.

Sensor set-ups for laser welding typically consist of an optical fibre collecting process emissions and guiding them to photodiodes which converts them into a time dependent voltage signal, which will be amplified and digitalized by an A/D-converter. A DSP or a computer carries out signal analysis, enabling us to create threshold rules that distinguish between defect and no defect welding. The thermal emissions from the process contain a lot of information about the process dynamics, like melt pool motion, which is very difficult to interpret.

While cameras are suitable for visualisation and for sophisticated measurement of e.g. the melt pool or keyhole dimensions, one or several photodiodes are powerful for simpler, industrial robust monitoring of the process. The signal integrates the emitted information from the process and this makes it more difficult to interpret, requiring empirical correlations with welding defects or a theoretical understanding of the process, which is limited today. Many researchers studied this type of sensor successfully [17-23]. Bagger and Olsen [17] placed a single photodiode under the weld zone. The system successfully controlled the power of the laser to achieve full penetration in sheets of variable thicknesses. Using single diodes is also used by Sanders [24], but they have gone a step further by using the signal to detect part misalignment and surface contamination. Ghasempoor et al [18] used three diodes, one for UV, one for IR and one for visible light. By using this setup they have detected lack of fusion and also, in some cases, porosity.

The photodiode can also be combined with other sensing techniques like voltage and current signals in hybrid welding. Using this method Tönshoff [19] detected lack of fusion and porosity defects. Observation of hybrid welding by photodiodes has been carried out by Travis [27], showing that a simple and cheap system can be effectively used. Different sensor combinations were tried by Sun [21] who demonstrated the use of acoustic sensors for monitoring of both solid based and airborne sound emissions. These were combined with UV and IR sensors to detect if the weld had penetrated fully or not.

If access to the process zone is difficult, fibre optics can be employed, later splitting the signal to different sensors. This method of measuring has been used by Chen [20]. A combination of a variety of sensors provided good insight in the process as Bad'yanov [23] has done by using IR, UV and temperature diodes together with a pyrometer and a CCD camera. They accomplished a suitable mathematical approximation of the signals and consequently lowered the signal computation efforts. The photodiode is successfully used in heavy industry when welding thick plates [18, 26]. **Fig. 6(a)** shows the correlation between the photodiode signal and full or partial weld penetration, respectively.

Visualisation of the weld pool is performed by CMOS-cameras, requiring less signal interpretation, but involving image evaluation processing, which is more straightforward. Several authors studied the setup with photodiode and camera. Kawahito et al have come a long way in introducing adaptive control to laser spot welding [22]. Several system manufacturers have developed mature systems on the market, i.e. Weldwatcher [28], Fraunhofer ILT CPC [29], Precitec [30] and Prometec [31]. Single pictures can be isolated from the camera, correlating to different situations during welding. This has been studied by Bardin [32], monitoring the penetration depth in real time with a photodiode and analysing the pictures from the camera to be able to control the penetration depth.

<ins>Pyrometer sensor:</ins> The process can also be monitored by employing a pyrometer, as used by Doubenskaia [33-35] and Bertrand [36]. They use the pyrometer to monitor the surface temperature for different setups like laser cladding [33], not for monitoring of defects but for optimisation of cladding parameters. In [34] a

pyrometer monitors the surface temperature profile during a laser pulse, e.g. to control how the melt is formed to avoid thermal decomposition of sensitive materials. The pyrometer can also be used to monitor weld quality during welding of zinc coated steels. This can be effective as the quality of these welds are connected to the joint gap, and the gap gives different temperatures depending on its size [35]. Bertrand [36] uses a pyrometer to detect fusion defects and lack of shielding gas, as well as variable speed and gap misalignment, see **Fig. 6(b)**.

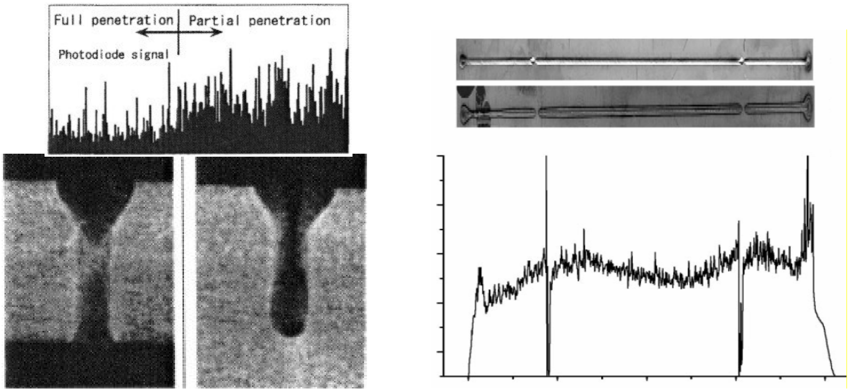

Fig. 6: ***(a)*** *Photodiode signal detecting full vs. partial weld penetration [26];* ***(b)*** *pyrometer signal detecting laser weld interruptions [36]*

Other sensors: More unusual monitoring techniques have been studied by several authors [37-42]. Earlier, Weerasinghe [37] and Gu [38] used acoustic emission sensors to monitor the lack of penetration or the penetration depth. Li [41] compared two different ways of monitoring with acoustic emission sensors.

Hand et al [39] looked at the plasma radiation reflected through the cladding layer of the optic fibre that guides the laser beam. They successfully detect focus errors and shield gas interruption during welding. A similar method of monitoring using the fibre delivery system is presented by Baik et al [40], however they use so-called chromatic filtering to detect power variations and focus shifts. They measured the thermal radiation of the melt pool at different wavelengths and then identified mathematical correlations to calculate the focus shift and power variation. Another way of monitoring the welding process is to measure the plasma charge. Li [41,42] measures the charge between the nozzle and the work-piece during keyhole welding, enabling the detection of keyhole failure, penetration depth, weld perforation, crater formation, weld humping, gap and beam position shift.

Weld defects, monitoring techniques and ways of controlling the process of welding have been reviewed by various authors. Kessler [43] describes pre-, in and post-process monitoring different defects and how to effectively monitor them using two different methods. Wiesemann [44] took an in-depth look at process monitoring for many different laser techniques. He describes what sensors to use with different methods. Shao and Yan [45] surveyed on-line monitoring techniques for laser welding, classifying the sensors into acoustic, optic and other types.

5.3 Digital Signal processing

Supervision of, and fault detections in, laser welding is an area of great importance within both the academic world and also within manufacturing industry. The main parameters of interest are penetration depth, heat affected zone (HAZ), pore and crack formation. The measurable parameters are shown and summarized in the picture below.
This section is a survey of how Digital Signal Processing algorithms have been used for supervision and fault detection within research and industry. It consists of three main sections covering; traditional time and frequency domain methods, neural nets and fuzzy logic and statistical modelling methods.

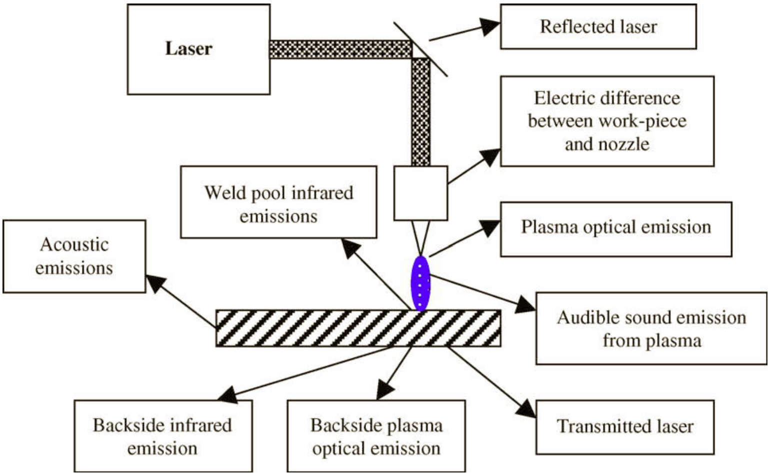
Laser
Reflected laser
Electric difference between work-piece and nozzle
Weld pool infrared emissions
Plasma optical emission
Acoustic emissions
Audible sound emission from plasma
Backside infrared emission
Backside plasma optical emission
Transmitted laser

Fig 7. Monitorable emissions from laser welding - Luoa [50]

5.3.1 Time domain analysis

Regarding signals in time, this survey is limited to measurements of emissions from the plasma cloud during CO2 welding and to acoustic emissions from the weld.

One overall problem in welding supervision is the often poor signal to noise ratio. In non-stationary processes, many features overlap both in time and frequency domain and are therefore are inseparable in the measured signal. Signals from e.g. the edges of the work piece can also overlap the desired signal but will not give any information about the welding process itself.

a. Emissions from the plasma cloud in CO2 welding.

A common and straightforward method is to monitor the plasma temperature using photodiode sensors, and apply a tolerance band on the signal, based upon the history of several successful runs of a particular weld. Defects are then detected when the signal goes outside this tolerance band.
Examples of this approach can be found in e.g. Kessler [43] and Prometec[46].
Also Tönsdorff[47] proposes a dynamic threshold for fault detection. Tönsdorff also describes the approach of identifying process parameters as a feature vector,

clustering these feature vectors and define boundaries between them as a way to separate defect welds from non defect welds.

b. Acoustic emissions from the workpiece.

Several authors have implemented feature extraction algorithms using e.g. matched filter approaches, or wavelet analysis of the received signal.

One way to accomplish this feature extraction is to resolve the signal using wavelet transforms. Wavelets are orthogonal sets of time scaled and time shifted waveforms. These kinds of transforms have an advantage in being able to localize events in the time domain as opposed to Fourier or Laplace transforms.

Kercel et.al. [48] investigated several methods to detect weld defects in tailored blanks welded with both Nd:YAG and CO2 lasers. In their work they used a separate pulsed laser to induce acoustic waves downstream the weld in the work piece (in this case tailored blanks) and the goal was to identify signal patterns for good welds and defective welds in the reflected signal.

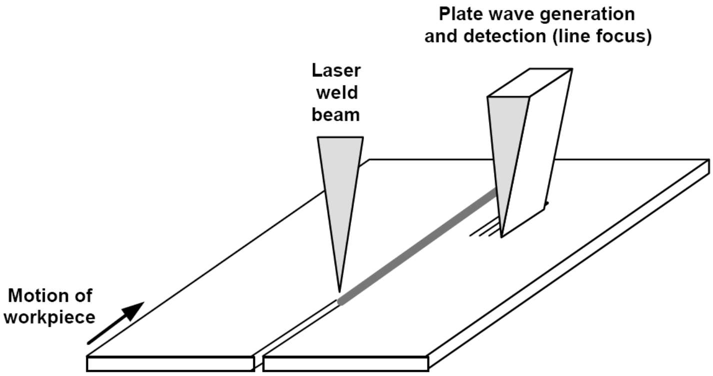

Fig 8 Laser induced acoustic waves. From [48]

The goal here was to separate the desired signal from the noise and irrelevant signals and still maintain the desired information.
As an initial technique to see if this approach would be fruitful, Kercel first resolved the detected signal into a set of four distinct Gabor wavelets plus additive Gaussian noise (without time scaling).
(Gabor wavelets can be seen as damped sinuses)
Another reason for choosing a fixed set of Gabor kernel functions is that this approach reduces the computational burden significantly compared to a full time/frequency wavelet analysis.

Kercel found this approach promising and later used a set of 960 Daubechies wavelets [49] for the final tests and found that the first 8 coefficients normally contained about 96-97% of the signal energy (bias) and the 900 smallest coefficients contained mainly noise and that information about pinhole defects could be found in the region between these.

5.3.2 Frequency domain analysis

In this section we cover both traditional frequency analysis (like FFTs) and also methods better suited for analysis in both time and frequency domain e.g. wavelet analysis, even though the name frequency normally refers to sinusoidal signals and wavelets are neither necessary nor normally sinusoidal in shape.

A good introduction to the use of wavelets in laser welding supervision can be found in Zeng et.al [52]. Zeng used wavelet techniques to decompose the signal into different sub-bands before training a neural net.

5.3.3 CO2 welding using audible signals

Both Hongping and Duley [53] and Zeng [52] have found that the spectrum from emitted sound contains information in the 10Hz - 20 kHz range during welding of mild steel.

They used an intensity modulated beam and found that good welds showed more discrete spectral components with harmonics of the modulation frequency compared to defective welds which gave a more smeared spectra. The same tendency could also be seen in spectra from welding with unmodulated beams, i.e. a more discrete spectrum from good welds. These oscillations were explained as coming from the material itself. Is has also been found that the spectra from keyhole welding contains more high frequency components than conduction welding. Oscillations in the range of several hundreds kHz was found originating from the keyhole itself – which can be seen as acting like an “organ-pipe”.

Hongping [51] also showed that if the emitted acoustic spectra from a CO2 weld were divided into 20 distinct bands of 1 kHz each, it was possible to discriminate between overheated, fully penetrated and partially penetrated welds by using Fisher discrimination analysis [64]

5.3.4 Neural nets and fuzzy logic

Studies of the feasibility of neural nets, as tools for fault detection and classification, have been carried out by several authors like e.g. Bollig et al [55] and Jeng et.al. [56]. In general the nets used have been of standard MLP (Multi Layer Perception) types trained by back propagation (BP) algorithms.

Luoa [50] decomposed the audio signal into 7 wavelet components where these components were used to train both a three-layer net as well as a simpler single- layer net, both trained with BP.

The conclusion was that a properly chosen and trained net could discriminate between a good weld and an error like a gap, but also that the task of choosing the proper net type and training algorithms and sets is an important but tedious task (which is a known fact in neural net theory).

Kwon et. al. [57] managed to discriminate between good and defective CO2 welds with a success rate of 93% using a three-layer MPL.
Sun et.al. [58] used the FFTs from audible sound (AE) emissions, Ultra violet (UV) and audible sound (AS) from CO2 weldings as inputs for feature extraction. Four methods were investigated and compared:

- Singular Value Decomposition (SVD).
- Class Mean Scatter (CMS)
- Decision fusion with SVD
- Decision fusion with CMS

For PCA and SVD see e.g. Oja [59] or Fausett [60]. A good introduction to neural nets can be found in Haykin [61]

5.3.5 Statistical signal processing methods

In Statistical Signal Processing the received signal is modelled as an output from a system where some of the systems state variables can be physical properties, hidden factors, measurable or immeasurable quantities. Within this field fall methods like Kalman filtering, change detection, optimal filtering, (Maximum Marginalized Likelihood) MML and (Maximum Generalized Likelihood) MGL estimation.

System identification

Bollig et. al. [55] have shown a way to build a ‘one step ahead’ predictor for estimating penetration depth.
For this they modelled the welding process as a NARX-model (Non-linear Auto Regressive, eXogenous input) using speed v and laser power p as inputs, the plasma intensity I as the controlled variable together forming a regression vector φ and finally penetrations depth D as an immeasurable state variable. The regression vectors from time i were used to train a MLP with 10-neurons in the hidden layer. Later they also implemented a 25 step ahead predictor.

Kaierle et.al. [62] modelled the welding process as a dynamic system using system identification methods to control weld depth using input power as the controlled variable and the front of the weld pools as the observed variable.

ICA and BSS methods for source separation.

Not much work has been carried out in this area, except for one interesting approach made by the colour research group at Joensuu University regarding the separation and identification of independent signal components from colour spectra measurements from CO2 welding using Independent Component Analysis (ICA) [59] and Principal Component Analysis (PCA) [61].

Change detection

The name change detection in this case refers to methods for identifying a change in for instance the mean or variance of a signal and the most probable time of event for

this change. A good introduction to this field can be found in Gustafsson [63] and Kay [64].
In this paper we are looking at attempts to detect statistical changes like a change in the mean or variance in signals normally heavily disturbed by noise, mostly of which is of Gaussian or Poisson kind.

The references for this section are listed in Section 9

5.4 Conclusions

The detection or suppression of laser welding defects is essential for successful welding applications. A series of different welding defects can be distinguished. Their physical origin is often only partially understood. According to the survey presented here, high speed imaging and mathematical modelling are powerful methods for improved understanding. Nevertheless, as a result of the complexity of the process, only parts of the underlying mechanisms have so far been revealed. Also mathematical modelling of the resulting fracture mechanisms has been conducted.

In-process monitoring of electromagnetic or acoustic emissions by different sensors enables access to information on the process dynamics related to the generation of welding defects. Cameras provide images of the top weld pool and keyhole geometry, while photodiode sensors and pyrometers provide more abstract, but industrially more powerful monitoring. Today mainly empirical correlations between sensor signals and defects have led to suitable industrial applications, and there is still a strong need for better understanding of the process-signal correlation and in turn for more systematic monitoring.

Regarding the signal processing part: The general impression is that in the articles little is said about why a particular method is chosen and what the goal was and how well the method chosen fulfilled these goals. A suggestion for future research is to focus on the statistics of the measured signals and after that, system identification or neural nets can be more properly trained from the start.

6. Summary of the papers

In this section the abstract and conclusions of the six papers of the thesis are presented.

Paper I

Title

State of the art of monitoring and imaging of laser welding defects.

Abstract

Several weld defects such as lack of fusion, blow-out holes, porosity, cracks and undercut can occur during laser welding. These defects can be crucial for product failure. Due to its complexity, the laser welding process and the origin of its defects are only partially understood. Both experimental observation and numerical simulation is difficult. Generally accepted knowledge of welding defects together with high speed imaging, X-ray transmission, and mathematical modelling have generated some understanding. However, experimental observation suffers from problems such as the small size of the process zone, its highly dynamic nature and the hot environment. In addition, the physical process is too complex for complete simulations.

As well as avoiding welding defects through process understanding, detection is of importance in industrial production. Monitoring can be divided into pre-, in- and post-process inspection, and between on- and off-line. Off-line post inspection is often expensive. Nowadays in-process monitoring is provided by photodiodes or cameras, but owing to the lack of fundamental process understanding, it is limited to empirical correlations between the appearance of a defect and signal changes.

The present review provides a survey on laser welding defects, on their experimental observation, on their theoretical treatment by modelling or simulation and on their detection by process monitoring. Despite wide ranging research efforts, the understanding and detection of laser welding defects is still very limited and unsatisfactory, and this hinders industrial implementation. Further research will be needed to fully control this critical welding process and in turn to guarantee reliable production and safe product function.

This survey is also considers methods for laser welding supervision from a Digital Signal Processing point of view. Both traditional 1-dimensional time or frequency domain methods as well more recent statistical and neural net approaches are covered.

Conclusions

The detection or suppression of laser welding defects is essential for successful welding applications. A series of different welding defects can be distinguished. Their physical origin is often only partially understood. According to the survey presented here, high speed imaging and mathematical modelling are powerful methods for improved understanding. Nevertheless, as a result of the complexity of the process, only parts of the underlying mechanisms have so far been revealed. Also mathematical modelling of the resulting fracture mechanisms has been conducted.

In-process monitoring of electromagnetic or acoustic emissions by different sensors enables access to information on the process dynamics related to the generation of welding defects. Cameras provide images of the top weld pool and keyhole geometry, while photodiode sensors and pyrometers provide more abstract, but industrially more powerful monitoring. Today mainly empirical correlations between sensor signals and defects have led to suitable industrial applications, and there is still a strong need for better understanding of the process-signal correlation and in turn for more systematic monitoring.

Regarding the signal processing part: The general impression is that in the articles little is said about why a particular method is chosen and what the goal was and how well the method chosen fulfilled these goals. A suggestion for future research is to focus on the statistics of the measured signals and after that, system identification or neural nets can be more properly trained from the start.

Paper II

Title
Advances in pulsed laser weld monitoring by the statistical analysis of reflected light.

Abstract

This paper describes two new techniques for monitoring the quality of laser welds by statistical analysis of the reflected light signal from the weld surface. The first technique involves an algorithm which analyses the variance of the peak values of the reflected signal as a measure of the stability of the surface during pulsed Nd:YAG laser welding in the heat conduction mode. Kalman filtering is used to separate a useful signal from the background noise. A good correlation between weld disruption and signal fluctuation has been identified. This technique could be used in tandem with the present practice of simply using the peak values of the reflected (or emitted) light as an indicator of weld quality. The second technique investigated involves an assessment of the temporal shape of the power distribution of individual reflected pulses in comparison with an average of the results from a high quality weld. Once again, a high correlation between a poor signal match and inferior quality welding was discovered, which may pave the way towards a new generation of optical weld monitoring devices.

Conclusions
Kalman filtering is a superior method to cut-off filtering for extracting data from noisy signals.

Signal variance data can be used in conjunction with raw signal data to improve the sensitivity and robustness of laser welding monitoring devices.
Reflected pulse shape comparisons involving polynomial best fits are a very promising tool for on-line process monitoring for pulsed laser welding.

Paper III

Title

Challenges to the Interpretation of the Electromagnetic Feedback from Laser Welding

Abstract

This paper considers the point that it is not possible to interpret individual weld perturbations from the raw electromagnetic feedback collected from laser weld zones. The presentation of electromagnetic data as a 3D cloud is presented as a new, useful tool in the analysis of this feedback. For example, it is shown that there is a very low correlation between the plasma or thermal signals and the reflected light signal from the weld zone, and that a strong correlation exists between the plasma and thermal signals. It is also demonstrated that data points from a weld perturbation form a different 3D cluster to those from the stable welding process. A strategy for future on line data analysis is presented in the use of a suitably shaped data cloud envelope. The rates of data fit to the various segments of such an envelope could be correlated with specific weld anomalies.

Conclusions

- It is not possible to interpret individual weld perturbations from the raw electromagnetic data collected from laser weld zones.

- The presentation of electromagnetic data as a 3D cloud provides a new, useful tool in the analysis of feedback from laser weld zones.

- There is a very low correlation between the plasma or thermal signals and the reflected light signal from the weld zone.

- There is a strong correlation between the plasma and thermal signals from the weld zone.

- Data points from a weld perturbation (blow out) form a different 3D cluster to those from the stable welding process.

- A strategy for future on line data analysis is the use of a suitable data cloud envelope or multi-layered envelopes. The rates of data fit to the various segments of such envelopes could be correlated with specific weld anomalies.

Paper IV

Title

Ripple formation on the surface of laser spot welds

Abstract

During laser spot welding of titanium surface ripples were found to originate from melt pool oscillations. The combination of oscillation in the melt pool and a fast solidification froze the oscillations as ripples on the surface. The solution to the problem was to delay the solidification until the oscillations were dampened out. By pulse shaping, ripple free weld spots were created.

Conclusions

In the latter stages of the laser-melt interaction during pulsed laser spot welding, the central portion of the weld is depressed as a result of localised boiling which exerts a pressure on the melt. As the laser pulse ends, the boiling ceases, and the pressure is removed. The melt then begins to return to its equilibrium geometry under the influence of surface tension, but the vertical momentum of the melt carries it past this equilibrium position. The surface then experiences damped simple harmonic motion. Ripples on the surface of the solid welds are created by rapid solidification of a surface which was undergoing damped simple harmonic motion. By delaying the solidification until the harmonic motion is completely dampened, surface ripples can be avoided.

7. Conclusions

This work has shown that it is possible by to detect deviations from stable weld behaviour by monitoring e.g. reflected laser light from the process, and in certain cases discriminate between different defects like gaps and unstable welds using a simple 1D-sensor and DSP-algorithms.

The use of high speed imaging has on one hand led to deeper insight into the dynamics and behaviour of welding processes and on the other hand where this imaging has been used in conjunction with simultaneous measurements and DSP-algorithms made it possible to directly couple actual weld behaviour to patterns in the received signals.

8. Future work

Interdisciplinary collaboration between Laser Physics, Metallurgy and Digital Signal Processing has shown itself to be prosperous in this work, so continuing this kind of cooperation is recommended to move the knowledge base and the possibilities forward towards more robust and intelligent supervision techniques.

Also a thorough investigation on different metals of the algorithms presented here would be of great interest to test the validity of the presented, in conjunction with using different laser sources and wavelengths.

For a more complete understanding of the factors determining weld quality and the interaction between weld pool behaviour, radiated optical emissions and signal shape, more work on the mathematical modelling of the laser to metal interaction and radiation to sensor/signal behaviour is needed.

Other factors that have showed good potential are to incorporate analysis of the emitted weldpool spectrum into supervision algorithms and to use e.g. PCA or multidimensional wavelets to decompose the weldpool surface into distinct orthogonal sub functions.

In the DSP field there are also numerous approaches of interest that can be applied. Because the received signal form a sensor often is disturbed by, or mixed with, information from other signal sources, a setup a multisensor environment with several sensors mounted physically apart enabling the use of ICA (Independent Component Analysis), BSS (Blind Source Separation) would be of interest. Also to continue the work already done by several groups to apply various Neural Networks and Fuzzy logic methods is a way forward.

Finally, of course one must mention Image processing where lots of information about the process is possible to extract.

9 References

1. -, Swedish standard, SS-EN ISO 13919-1, p. 27 (1996)
2. A. Matsunawa, S. Katayama, **Understanding physical mechanisms in laser welding for construction of mathematical models**, Welding in the World, Le Soudage Dans Le Monde, v 46, n SPEC, p 27-38 (2002)
3. E. H. Amara, R. Fabbro, F. Hamadi, **Modeling of the melted bath movement induced by the vapour flow in deep penetration laser welding**, Journal of Laser Applications, v 18, n 1, p 2-11 (2006)
4. R. Fabbro, S. Slimani, I. Doudet, F. Coste, F. Briand, **Experimental study of the dynamical coupling between the induced vapour plume and the melt pool for Nd:YAG CW laser welding**, J. Phys. D: Applied Physics, v 39, n 2, p 394-400 (2006)
5. R. Fabbro, S. Slimani, F. Coste, F. Briand, **Study of keyhole behaviour for full penetration Nd:YAG CW laser welding**, Journal of Physics D: Applied Physics, v 38, n 12, p 1881-7 (2005)
6. X. Jin, P. Berger, T. Graf, **Multiple reflections and Fresnel absorption in an actual 3D keyhole during deep penetration laser welding**, Journal of Physics D: Applied Physics, v 39, n 21, p 4703-12 (2006)
7. A. F. H. Kaplan, M. Mizutani, S. Katayama and A. Matsunawa, **Unbounded keyhole collapse and bubble formation during pulsed laser interaction with liquid zinc**, Journal of Physics D: Applied Physics, v 35, p 1218-1228 (2002)
8. K. Nishimoto, H. Mori, **Hot cracking susceptibility in laser weld metal of high nitrogen stainless steel**, Sci. Techn. Adv. Mat., v 5, p. 231-240 (2004)
9. J. F. Gould, S. P. Khurana, T. Li: **Predictions of microstructures when welding automotive advanced high strength steel**, Weld. J., v 85, p 111s-116s (2006)
10. S. Hao, W. K. Liu, B. Moran, F. Vernerey, G. B. Olson, **Multi-scale constitutive model and computational framework for the design of ultra-high strength high toughness steels**, Comput. Meth. Appl. Mech. Eng, v 193, p 1865-1908 (2004)
11. U. Prahl, S. Papaefthymiou, V. Uthaisansuk, W. Bleck, J. Sietsma, S. van der Zwaag, **Micromechanics-based modelling of properties and failure of multiphase steels**, Comp. Mat. Sci, v 39, p 17-22 (2007)
12. www.redlake.com
13. www.pco.de
14. www.dantecmt.com
15. www.photron.com

16. A. Fellman, A. Salminen, V. Kujanpää, **A study of the effects of parameters on filler material movements and weld quality in CO_2-laser-MAG hybrid welding**, (NOLAMP10 2005), Luleå, p343-354, (2005)
17. C. Bagger, F. O. Olsen, **Laser welding closed-loop power control**, Journal of Laser Applications, v 15, n 1, p 19-24 (2003)
18. A. Ghasempoor, P. Wild, M. Auger, R. Mueller, **Automatic detection of lack of fusion defects in CO2 laser gear welding**, J. Laser Appl., v 15, n 2, p 77-83 (2003)
19. H. K. Tönshoff, K. Körber, T. Hesse, M. Stallmach, **Increased performance and flexibility of process monitoring for deep penetration laser welding**, ICALEO 2002. 21st Intl. Congress on App. of Lasers and Electro-Optics, p 1105-13 Vol.2 (2002)
20. H.B. Chen, L. Li, D.J. Brookfield, W.M. Steen, **Multi-frequency fibre optic sensors for in-process laser welding quality monitoring**, NDT&E International, v 26, n 2, April 1993, p 67-73 (1993)
21. A. Sun, Elijah Kannatey-Asibu, Jr., **Monitoring of laser weld penetration using sensor fusion**, Journal of Laser Applications, v 14, n 2, p 114-21 (2002)
22. Y. Kawahito, Seiji Katayama, **In-process monitoring and control for stable production of sound welds in laser microspot lap welding of aluminium alloy**, Journal of Laser Applications, v 17, n 1, p 30-37 (2005)
23. B.N. Bad'yanov, A.A. Elizarov, **Application of the step by step approximation method for the computer control of laser welding processes,** Measurement Techniques, v 46, n 2, p 162-5 (2003)
24. P. G. Sanders, J. S. Keske, K. H. Leong, G. Kornecki, **Real-time monitoring of laser beam welding using infrared weld emissions**, J. Laser Appl., v 10, p 205-11 (1998)
25. K. Kamimuki, T. Inoue, K. Yasuda, M. Muro, T. Nakabayashi, A. Matsunawa, **Prevention of welding defect by side gas flow and its monitoring method in continous wave Nd:YAG laser welding**, J. Laser Appl., v 14, n 3, p 136-145 (2002)
26. K. Kamimuki, T. Inoue, K. Yasuda, M. Muro, T. Nakabayashi, A. Matsunawa, **Behaviour of monitoring signals during detection of welding defects in YAG laser welding. Study of monitoring technology for YAG laser welding**, Q. Journal of the Japan Welding Society, v 20, n 3, August, 2002, p 369-377 (2002)
27. D. Travis, G. Dearden, K. G. Watkins, E.W. Reutzel, R.P. Martukanitz, J.F. Tressler, **Sensing for monitoring of the laser GMAW Hybrid welding process**, ICALEO 2004. 23rd International Congress on Applications of Lasers and Electro-Optics, (2004)
28. S. Postma, R.G.K.M. Arts, **Penetration control in laser welding of sheet metal**, Journal of Laser Applications, v 14, n 4, p 210-214 (2002)

29. J. Petereit, P. Abels, S. Kaierle, C. Kratzsch, E.W. Kreutz, **Failure recognition and online process control in laser beam welding**, ICALEO 2002. 21st International Congress on Applications of Lasers and Electro-Optics, pt. 4, p 2501-9 Vol.4 (2002)
30. M. Kogel-Hollacher, T. Nicolay, A. Kattwinkel, M. G. Muller, J. Muller, **On-line process monitoring in laser material processing-techniques for the industrial environment**, (PICALO 2004), LMP-SC, p 1-4, (2004)
31. J. Beersiek, **New aspects of monitoring with a CMOS camera for laser materials processing**, (ICALEO 2002), pt. 2, p 1181-90 Vol.2 (2002)
32. F. Bardin, A. Cobo, J. M. Lopez-Higuera, O. Collin, P. Aubry, T. Dubois, M. Högström, P. Nylen, P. Jonsson, J. D. C. Jones, D. P. Hand, **Optical techniques for real time penetration monitoring for laser welding**, Applied Optics, v 44, n 19, p 3869-76 (2005)
33. M. Doubenskaia, Ph. Bertrand, I. Smurov, **Optical monitoring of Nd:YAG laser cladding**, Thin Solid Films, v 453-454, p 477-85 (2004)
34. M. Doubenskaia, I. Smurov, **Surface temperature evolution in pulsed laser action of millisecond range**, Appl. Surf. Sci., v 252, n 13 SPEC. ISS., p 4472-4476 (2006)
35. M. Doubenskaia, Ph. Bertrand, H. Pinon, I. Smurov, **On-Line monitoring of Nd-YAG laser lap welding of Zn-coated steel sheets by pyrometer**, Proc. BTLA 2006, St. Petersburg (RUS), p 203-209, (2006)
36. Ph. Bertrand, I. Smurov, D. Grevey, **Application of near infrared pyrometry for continous ND:YAG laser welding of stainless steel**, Applied Surface Science, v 168, n 1-4, p 182-185 (2000)
37. V.M. Weerasinghe, J.N. Kamalu, R.D. Hibberd, W.M. Steen, **Acoustic signals from laser back reflection**, Optics and Laser Technology, v 22, n 6, p 381-6 (1990)
38. H.P. Gu, W.W. Duley, **A statistical approach to acoustic monitoring of laser welding**, Journal of Physics D: Applied Physics, v 29, n 3, p 556-560 (1996)
39. D.P. Hand, C. Peters, J.D.C. Jones, **Nd:YAG laser welding process monitoring by non-intrusive optical detection in the fibre optic delivery system**, Measurement Science & Technology, v 6, n 9, p 1389-1394 (1995)
40. S.-H. Baik, M.-S. Kim, S.-K. Park, **Process monitoring of laser welding using chromatic filtering of thermal radiation**, Meas. Sci. Technol., v 11, n 12, p 1772-7 (2000)
41. L. Li, **A comparative study of ultrasonic emission characteristics in laser processing**, Applied Surface Science, v 186, n 1-4, p 604-610 (2002)
42. L. Li, D. J. Brookfield, W. M. Steen, **Plasma charge sensor for in-process, non-contact monitoring of the laser welding process**, Measurement Science & Technology, v 7, n 4, p 615-626 (1996)
43. B. Kessler, **Online quality control in high power laser welding**, White paper, Precitec KG, Germany, 2003
44. W. Wiesemann, **Process monitoring and closed loop control**, Landholt-Börnstein – Group VIII Advanced Materials and Technologies, v 1C, Springer Berlin Heidelberg, XVIII, p 243-275, ISBN 978-3-540-00105-8, (2004)

45. J. Shao, Y. Yan, **Review of techniques for on-line monitoring and inspection of laser welding**, Journal of Physics: Conference Series, v 15, n 1, p 101-7 (2005)
46. "www.prometec.com."
47. H. K. Tonshoff, A. Ostendorf and W. Specker, "**Online monitoring and closed-loop control of laser welding processes**," vol. 1405. In Proc. of 12th international symposium for electromachining (ISEM), May 1998, pp. 603–612.
48. Stephen W. Kercel, Roger A. Kisnera, "**In-process detection of weld defects using laser-based ultrasound**," Oak Ridge National Laboratory, P.O. Box 2008, Oak Ridge, TN 37831-6011, Tech. Rep.
49. http://en.wikipedia.org/wiki/Daubechies_wavelet
50. Hong Luoa and Z. Zhoub, "**Application of artificial neural network in laser welding defect diagnosis**," Singapore Institute of Manufacturing Technology, 71 Nanyang Drive, Singapore 638075, Singapore bHuazhong University of Science and Technology, Wuhan 430074, PR China, Tech. Rep., June 2005.
51. W. D. Hongping. Gu, "**Discrete signal components in optical emission during keyhole welding**." ICALEO, 1997, pp. 40–46.
52. H. Zeng, Z. Zhou, Y. Chen, H. Luo, and L. Hu, "Wavelet analysis of acoustic emission signals and quality control in laser welding," Journal of Laser Applications, vol. 13, pp. 167–173, Aug 2001.
53. H. Gu and W. W. Duley, "**A statistical approach to acoustic monitoring of laser welding**," Journal of Physics D Applied Physics, vol. 29, pp. 556–560, Mar 1996.
54. J. R. A and W. D. W, **Applied Multivariate Statistical Analysis**. Englewood Cliffs, NJ: Prentice Hall, 1992.
55. C. S. A.Bollig, H.Rake, "**Application of neuro-predictive control to laser beam welding**," Institute of Automatic Control, Aachen university of Technology, Institute of Automatic Control, Aachen university of Technology, 52056 Aachen , Germany, Tech. Rep., 2002.
56. Jeng-Ywan Jeng and S.-M. Leuc, "**Prediction of laser butt joint welding parameters using back propagation and learning vector quantization networks**," Tech. Rep., 2000.
57. Jangwoo Kwon, Osang Kwon Younggun Jang, "**Development of neural network based plasma monitoring system for laser welding quality analysis**," TENCON, pp. 678–681, 1999.
58. M. G. Allen Sun, elijah Kannetey-Abisu Jr, "**Monitoring of laser weld penetration using sensor fusion**," Journal of laser applications, vol. 14, no. 2, pp. 114–121, May 2002.
59. A. Hyvarinen, J. Karhunen, and E. Oja, **Independent Component Analysis**. Wiley-Interscience, May 2001.

60. L. Fausett, **Fundamentals of Neural Networks**. Prentice-Hall, 1994, vol. ISBN 0-13-334186-0.
61. S. Haykin, **Neural Networks: A Comprehensive Foundation**. Prentice Hall, 1998.
62. Kaierle, S. Beersiek, "**Online control of penetration depth in laser beam welding**," vol. 3. Aachen,Germany: Industrial Electronics Society, 1998. IECON '98. Proceedings of the 24th Annual Conference of the IEEE, Sep 1998, pp. 1694–1698.
63. F. Gustafsson, **Adaptive Filtering and Change Detection**. John Wiley&Sons, 2000.
64. S. M. Kay**, Fundamentals of Statistical Signal Processing**. Prentice-Hall, 1998, vol. II

Paper II

Advances in pulsed laser weld monitoring by the statistical analysis of reflected light.

Advances in pulsed laser weld monitoring by the statistical analysis of reflected light.

R. Olsson[1,2], I. Eriksson[1], J. Powell[1] and A.F.H. Kaplan[1]
[1] Luleå University of Technology, SE-971 87 Luleå, Sweden; www.ltu.se/tfm/produktion
[2] Laser Nova AB, SE-831 48 Östersund, Sweden;

E-mail: rickard.olsson@lasernova.se; ingemar.eriksson@ltu.se; jpowell@laserexp.co.uk
Alexander.kaplan@ltu.se

Abstract

This paper describes two new techniques for monitoring the quality of laser welds by statistical analysis of the reflected light signal from the weld surface. The first technique involves an algorithm which analyses the variance of the peak values of the reflected signal as a measure of the stability of the surface during pulsed Nd:YAG laser welding in the heat conduction mode. Kalman filtering is used to separate a useful signal from the background noise. A good correlation between weld disruption and signal fluctuation has been identified. This technique could be used in tandem with the present practice of simply using the peak values of the reflected (or emitted) light as an indicator of weld quality. The second technique investigated involves an assessment of the temporal shape of the power distribution of individual reflected pulses in comparison with an average of the results from a high quality weld. Once again, a high correlation between a poor signal match and inferior quality welding was discovered, which may pave the way towards a new generation of optical weld monitoring devices.

1. Introduction

Several workers have attempted to use the light emitted and reflected from the laser welding process to predict the quality of the weld produced e.g. refs [1–4]. However, feedback systems in this field are always hampered by the high signal to noise ratios involved. Informative electromagnetic signals from the weld zone often overlap, both spatially and in their frequency range, with high levels of noise which carries no useful information. A thorough survey of commonly used monitoring methods can be found in [5].

The simplest and most common method of weld monitoring is to apply a tolerance band to a chosen electromagnetic signal (e.g. the plasma temperature or the reflected laser light from the weld zone), based on historic data of a repeated welding process. Defects are then associated with the signals which exceed this tolerance band. This approach is commonly applied to the monitoring of CO_2 laser welding in commercial devices [1,2] and in research [3]. Generally, a dynamic threshold for fault detection, which adjusts its value to gradual changes in signal level is employed, see fig. 1. In this paper the reflected signal from the weld pool to the sensor will be referred to as the 'R'signal. Kaierle [4] describes another approach; the monitored values from different parameters are grouped together as vectors and these 'feature vectors' are then allocated threshold values.

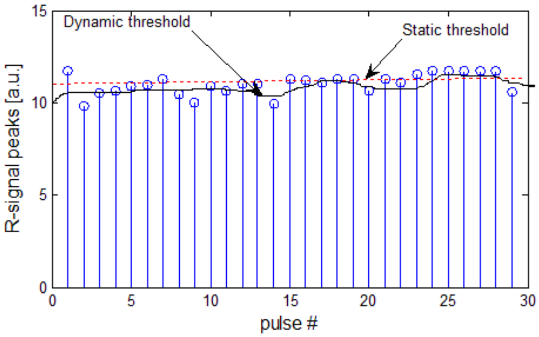

Figure 1. The usual method of weld monitoring would involve a threshold value for the observed signal. Dynamic thresholds, which self-adjust with time (e.g. solid line) are often more effective than static thresholds (e.g. dotted line).

However, in certain cases, the simple application of a tolerance band may not supply sufficient feedback about disruptions to the process. In this paper two different approaches to processing the data collected from a laser welding process are investigated. In the first, the variance of the peak values of the reflected light gives an extra dimension to the feedback from the signal received from the weld pool, and could be used in tandem with existing techniques to improve welding process control. The second technique involves the comparison of the temporal shape of the power profile of reflected pulses compared to an average 'high quality weld' reflected pulse. The results show great promise for the improvement of the performance of the next generation of laser welding monitors.

These two new statistical analysis techniques will now be discussed separately.

2. Analysis of the variance of the peak values of reflected pulses.

2.1 Description of the technique

For this research a new strategy was employed to overcome the problems associated with the high signal to noise ratio and at the same time introduce a computationally moderate approach enabling real time implementation. Rather than simply analysing the electromagnetic signals coming from the weld pool, the variance of those signals was analysed as follows;

A) Reflection data was collected from the weld zone using a pin diode at a sampling rate of 8 kHz this gave the raw data of the type shown in figure 2. The data shown here represents the power signal from one laser pulse reflected from the weld zone. A Kalman filter [6-9] was used to remove a lot of the noise from the signal, see fig. 3.

There are two reasons for the choice of Kalman filtering in preference to low pass filtering;

Kalman filters are the optimal linear estimator of a signal of a varying process whose measurements are disturbed by noise.

The signal from the reflected light exhibits such sharp peaks and edges it contains a considerable proportion of high frequency information. LP-filtering tends to smooth the peaks and thus disturb the measured signal shape.

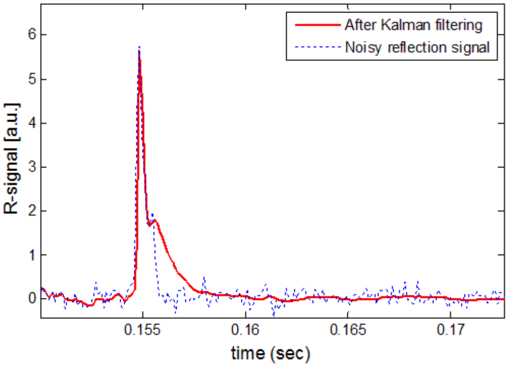

Figure 2. An example of the raw reflection data collected from a weld zone.

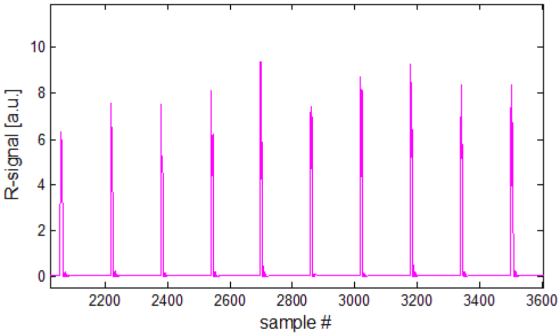

Figure 3. An example of Kalman filtered (noise reduced) reflection data collected from a weld zone.

B) The raw data was transformed by the CUSUM algorithm (see appendix 2), into simple peak power data – as shown in figure 4.

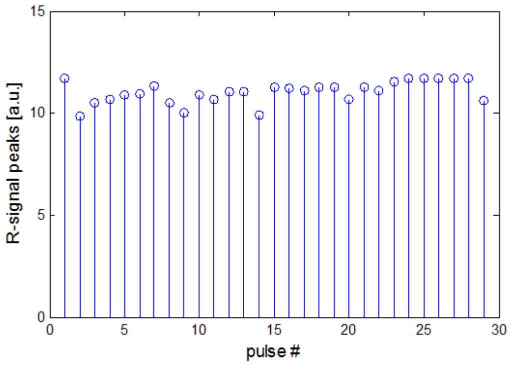

Figure 4. The raw data was simplified into peak values only.

C) The variance between the data peaks was calculated as each new peak (figure 4) was plotted. This gave clear information about perturbations in the welding process – see figure 5.

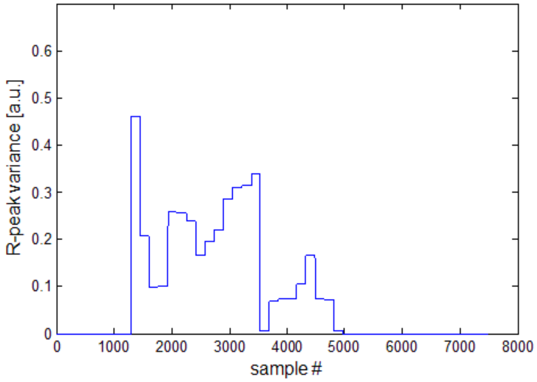

Figure 5. The variance of the peak values presented in figure 4.

The variance values of the type shown in figure 5 give valuable information about the stability of the process and this principle could be used in the design of the next generation of laser welding monitoring systems.

2.2 Experimental procedure

Three welds were prepared. In each case sheets of 0.14mm thick Inconel were mounted side by side and welded with an edge joint. For the first two welds the geometrical arrangement was that shown in figure 6 – the laser was aligned along the centre of the join line.

In the case of the first weld the welding parameters were set to give a stable welding process and a high quality weld – throughout this paper this will be referred to as the ‘stable’ weld.

The second weld was carried out under process parameters chosen to produce an unstable welding process and this weld will henceforth be referred to as the ‘unstable’ weld.

In order to test the statistical tools being used a third weld was produced which involved two faults in the weld geometry; a. The weld line was set at an angle to the interface of the two sheets and started on the edge of only one sheet and b. the two sheets were clamped together for the initial part of the weld but became gradually separated as the weld progressed. This complex geometry ensured that the weld would begin with one fault (misalignment to one side of the intended joint) and then become a stable, acceptable weld for a short time before ending with a different fault (weld failure through poor workpiece fit-up). This weld arrangement is shown in figure 7 and the resulting weld will be referred to as the ‘faulty’ weld during the course of this paper. The process parameters for all three welds are presented in table 1.

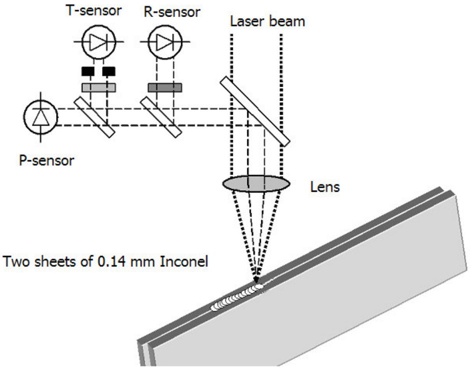

Figure 6 A schematic of the edge welding geometry for the ‘stable’ and ‘unstable’ welds.

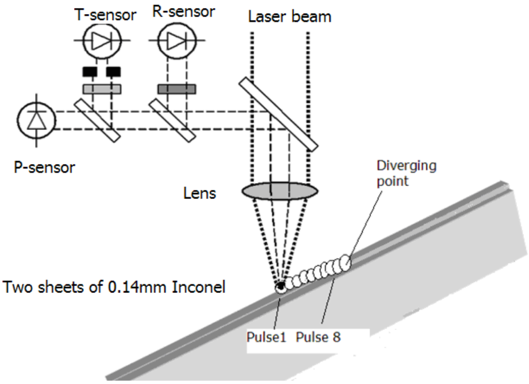

Figure 7 A schematic of the edge welding geometry for the 'faulty' weld. The weld begins on one workpiece only and then recovers its correct position before failing as a result of the gap between the workpieces.

Table 1 The process parameters for the three welds.

Weld name	Average Power (W)	Pulse Frequency (Hz)	Pulse Length (ms)	Pulse peak Energy (J)	Welding Speed (m/min)
Stable	70	50	1ms	1.6	0.3
Unstable	70	50	1ms	1.6	0.2
Faulty	70	50	1ms	1.6	0.3

The weld pool was illuminated by a Cavitar Cavilux Smart illumination system using a wavelength of 809nm and a peak power of several hundred Watts, in 1us pulses synchronized with the high speed camera. The process was filmed at 4000 fps with the Motion Pro X3 Camera.

Measurement data was converted into MatLab format for off line analysis and algorithm development. A real time implementation was made in LabView for simultaneous presentation of video and measurement data.

The sensor system consisted of Precitec LWM, Sensors for Plasma (P), Temperature (T) and Reflection (R) – with a sampling rate of 8 kHz.

3 Results and Discussion

Figure 8 is taken from the high speed imaging of the welding process. The photo shows the production of the stable, high quality weld. Figure 9 presents the reflection data collected during the production of this weld, together with a graph showing the variance of the peak values of the reflection data. With a laser pulse frequency of 50Hz and a sampling rate of 8 kHz. The pulses are very clear and well defined – and these reflection data graphs can be discussed with reference to either the pulse number or the sample number. It is clear from figure 9 that there is only a minor amount of variance in the reflection signal peaks in the case of this stable welding process

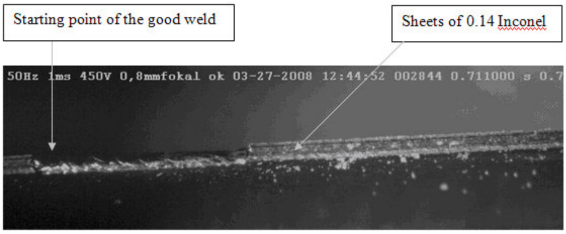
Starting point of the good weld
Sheets of 0.14 Inconel
50Hz 1ms 450V 0,8mmfokal ok 03-27-2008 12:44:52 002844 0.711000 s 0.7

Figure 8 A view of the stable weld

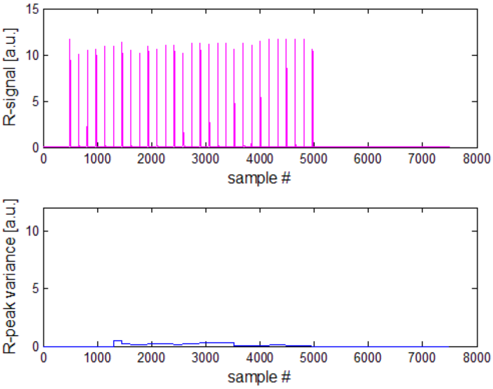

Figure 9. Data and Matlab calculations for the stable weld; 9a. Reflection data, 9b. Variance of reflection data peak amplitudes.

Figures 10 and 11 present similar data as figures 8 and 9 but, in this case for the unstable weld. In these results it is clear that the peak variance plot, figure 11b, involves larger values – indicating that the reflection signal, and the welding process which produced it, are unstable. The initial peak of the variance graph needs some explanation, as it is simply the result of the unusually high reflection signal from the first laser pulse. This pulse, see fig 11a, is larger than the others because the first pulse is the only one to encounter metal which is cold and therefore highly reflective. Subsequent laser pulses interact with liquid or recently solidified melt which has a lower reflectivity. The variance signal is calculated on a moving six point average and so no variance signal is provided until six pulses have been monitored. This first variance value is high simply because it includes the unusually energetic first pulse reflection.

In general however, the fluctuations in the reflected signal are a function of the fluctuations in the shape of the reflecting surface of the weld. The changes in melt surface geometry shown in the snapshots of figure 10 tend to give a reduced reflection signal but, occasionally, the disturbed melt surface provides a more effective reflector than a stable weld (as happened here in the third pulse from the end of the measurement). In some cases the surface of a poor quality weld might result in repeated high reflection values. In this situation a monitoring device based on a simple threshold might be misled into providing feedback that the process was continuing successfully. It is for this reason that a system designed around the variance of the signals might give additional, useful feedback.

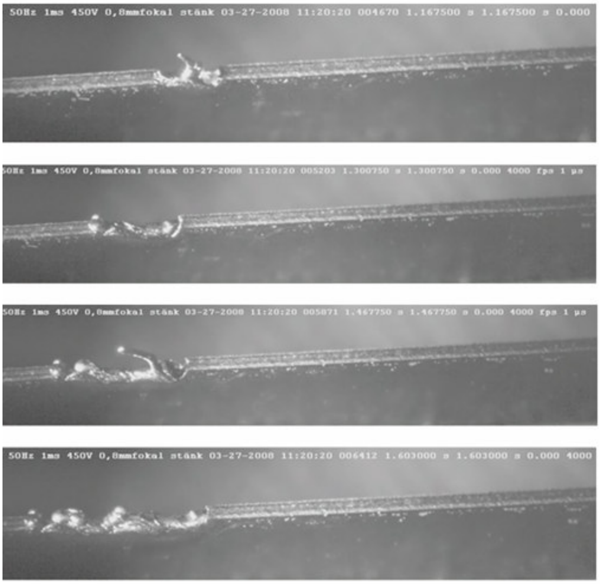
50Hz 1ms 450V 0,8mmfokal stånk 03-27-2008 11:20:20 004670 1.167500 s 1.167500 s 0.000
50Hz 1ms 450V 0,8mmfokal stånk 03-27-2008 11:20:20 005203 1.300750 s 1.300750 s 0.000 4000 fps 1 μs
50Hz 1ms 450V 0,8mmfokal stånk 03-27-2008 11:20:20 005871 1.467750 s 1.467750 s 0.000 4000 fps 1 μs
50Hz 1ms 450V 0,8mmfokal stånk 03-27-2008 11:20:20 006412 1.603000 s 1.603000 s 0.000 4000

Figure 10. An unstable weld after: (a) 0.167s Sample #1000; (b) 0.300s Sample #2000; (c) 0.467s Sample #3000; (d) 0.603s Sample #4800

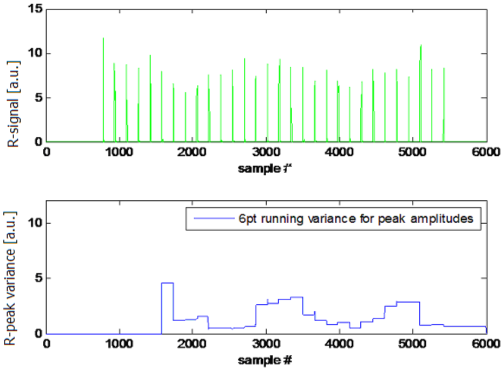

Figure 11.Data and Matlab calculations for an unstable weld; (a) Reflection data, (b) Variance of reflection data peak amplitudes.

Figure 12 is a snapshot taken from the high speed video of the production of the faulty weld just as the weld begins to encounter the gap between the two workpieces. Figure 13 gives the variance of the peak reflection values.

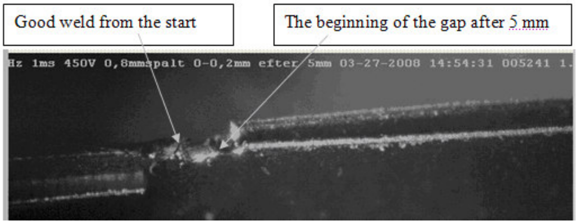
Good weld from the start
The beginning of the gap after 5 mm
Hz 1ms 450V 0,8mmspalt 0-0,2mm efter 5mm 03-27-2008 14:54:31 005241 1.

Figure 12 The start of the 'faulty' weld.

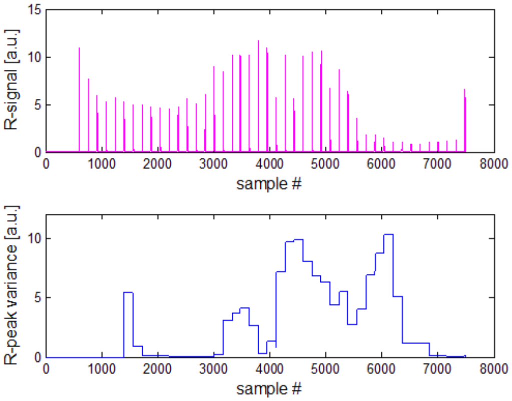

Figure 13. Data and Matlab calculations for the 'faulty' weld; (a) Reflection data, (b) Variance of reflection data peak amplitudes.

Figure 13 tells the complex story of the reflection data from the faulty weld which can be interpreted in the following way;

a. The first reflection, off the cold metal, has a high peak value.

b. The following dozen or so pulse reflections indicate a stable welding process with a much reduced peak value compared to the stable weld. This reduction in signal is due to the different geometry of the weld surface which is concentrated on one side of the join – one workpiece is experiencing only partial melting and thus the reflecting surface of the weld is reduced compared with the stable weld.

c. The reflected signal rises as the weld gradually involves the full width of both workpieces – in this zone the weld produced is similar to the stable weld.

d. From about sample 4000 the signal becomes very unstable as the weld geometry changes to accommodate the widening of the gap between the two workpieces.

e. Between samples 5000 and 6000 the reflected signal decreases to a very low value and remains low because the laser beam is no longer welding – it is simply passing into the gap between the two workpieces.

These results show that peak variance analysis can give information which is difficult to interpret in certain complex situations. However, in most cases welds can be classified as either stable or unstable, and it is suggested that peak variance analysis be included in the design of future weld monitoring equipment to achieve a more robust and sensitive feedback system.

4. Analysis of the temporal shape of the reflected pulses.

The following analysis utilises the same welds and data sets as the previous section but analyses the temporal power profile of the individual pulses rather than their peak values. Figures 14 – 16 present a new view of the original reflected pulses data set for the 'good', 'unstable' and 'diverging workpiece' welds. In each case the power profiles of the reflected pulses are presented using the x-(time) and z-(power) axes. The y-axis used to separate the pulses and display them as a sequence. It is clear from this basic data set that there are large differences in the repeatability of the pulse profiles for the stable and unstable welds.

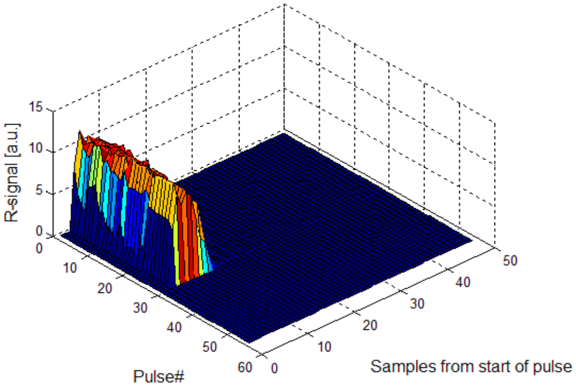

Figure 14. The basic data set for the 'good' weld. The power history for each reflected pulse is shown and the pulses are stacked next to each other as a sequence.

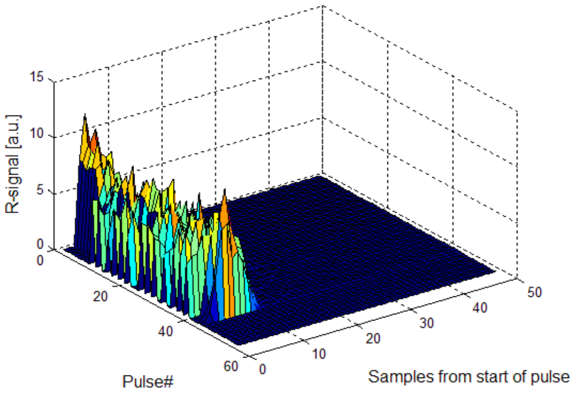

Figure 15. The basic data set for the 'unstable' weld. The power history for each reflected pulse is shown and the pulses are stacked next to each other as a sequence.

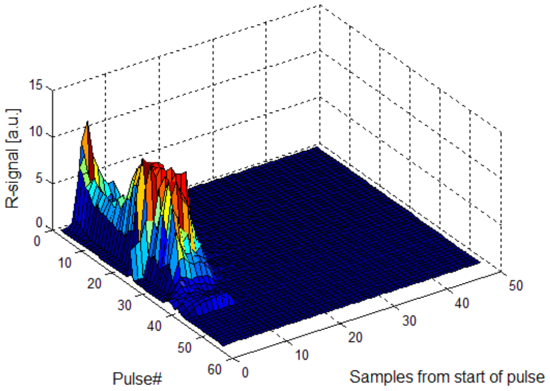

Figure 16. The basic data set for the 'faulty' weld. The power history for each reflected pulse is shown and the pulses are stacked next to each other as a sequence.

In order to establish a method of qualitative comparison between the data sets presented in figures 14 – 16 it is convenient to reduce the quantitative differences between the peak profiles by normalizing them all to the same maximum height. Comparisons between and within data sets can then be carried out without the extra complication of scaling factors. Figure 17 presents the same information as figure 14 with all the peaks normalised for height in this way.

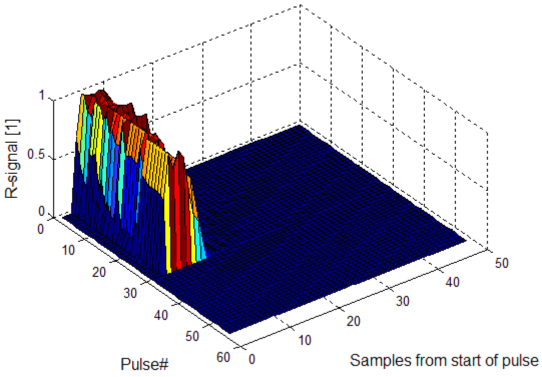

Figure 17. The basic data set for the stable weld – as in figure 14, but with all the pulses given the same maximum height.

With the data in this 'normalised height' form it is a simple matter to calculate the curve fit of a fourth order polynomial to the average pulse shape. This gives us a mathematical description of the average power profile of a reflected pulse from a satisfactory welding process. This polynomial fit is presented in figure 18.

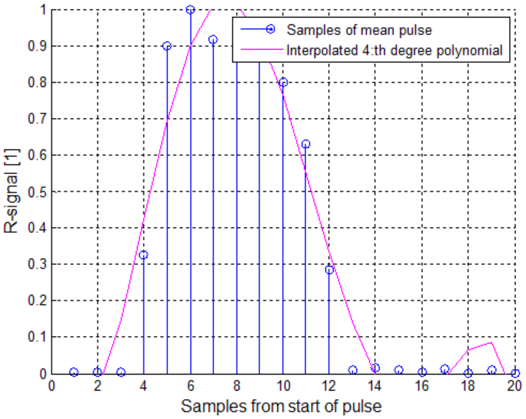

Figure 18.The polynomial fit of the average values of the temporal power profile of a reflected pulse from a satisfactory welding process.

If the polynomial curve in Fig 17 is denoted $p(t)$ then

$$p(t) = a_0 + a_1 t + a_2 t^2 + a_3 t^3 + a_4 t^4$$

In the case of these results;

$$a_0 = 0.4042, a_1 = -0.6815, a_2 = 0.3012,$$
$$a_3 = -0.0404, a_4 = 0.0021$$

I.e

$$p(t) = 0.4042 + 0.6815t + 0.3012t^2$$
$$-0.0404t^3 + 0.0021t^4$$

We can now compare the polynomial best fit for every pulse from each of our three welding situations to this mathematical template for a ‘good’ weld reflected pulse by looking at the values of the coefficients a1, a2, a3, and a4. Figures 19 and 20 present the height normalised results for the unstable and faulty welds, and figure 20 compares the values of the polynomial coefficients for all the pulses with the template in figure 18.

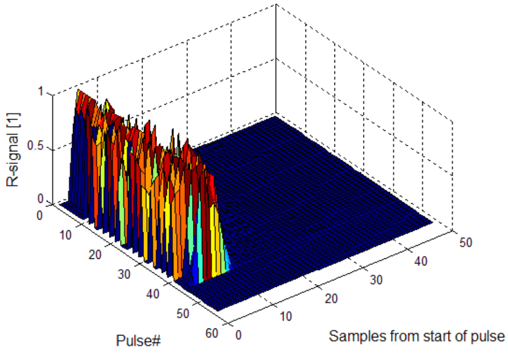

Figure 19. The basic data set for the ‘unstable’ weld – as in figure 15, but with all the pulses given the same maximum height.

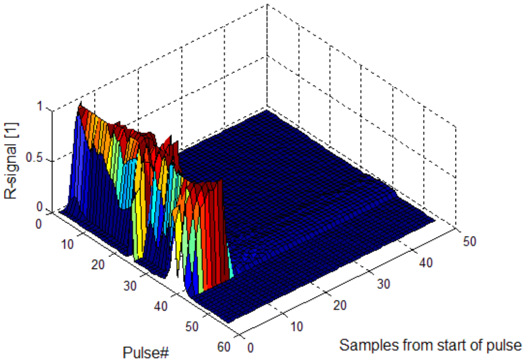

Figure 20. The basic data set for the ‘faulty’ weld – as in figure 16, but with all the pulses given

the same maximum height.

Figure 21 gives the expected result that the individual pulses have similar coefficients to the average pulse until the welding process ends after 21 pulses. Between pulses 21 and 30 the movement of the workpiece had stopped so the final pulses were fired into molten material

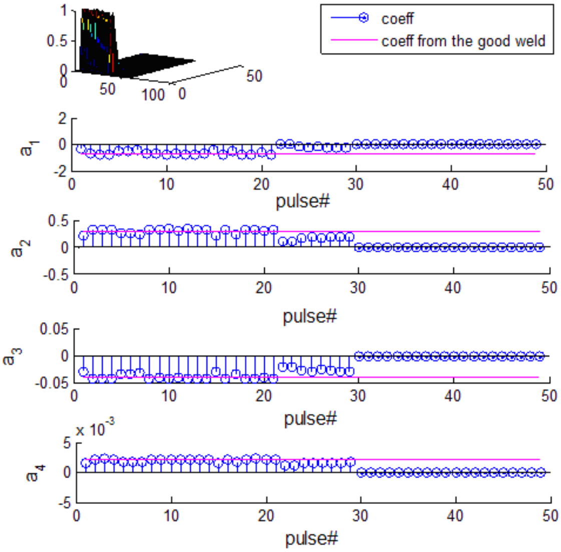

Figure 21 The values of the polynomial coefficients a_1, a_2, a_3, and a_4 for each pulse of the 'stable' weld.

Figure 22 shows that the instability of this weld is very clearly demonstrated in the variance of the polynomial coefficients and by the difference between the values involved and those of the stable weld average.

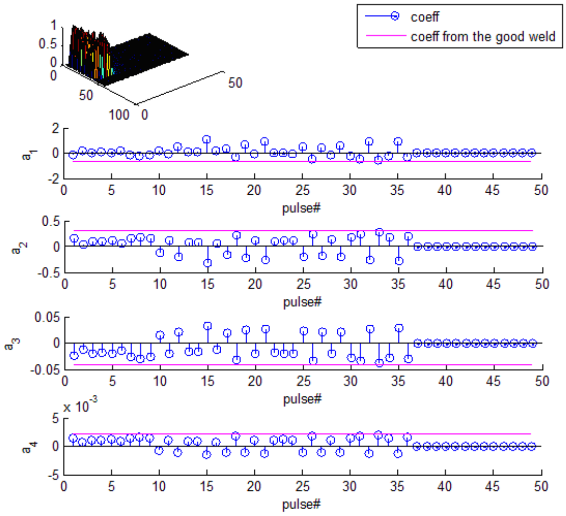

Figure 22 The values of the polynomial coefficients a_1, a_2, a_3, and a_4 for each pulse of the ‘unstable’ weld

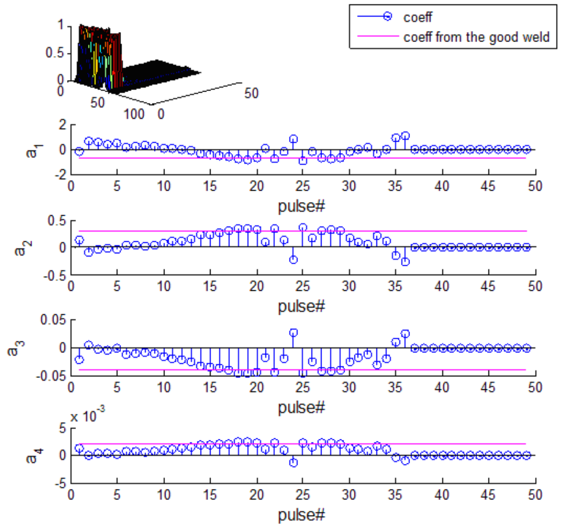

Figure 23 The values of the polynomial coefficients a_1, a_2, a_3, and a_4 for each pulse of the ‘faulty’ weld

The polynomial coefficients in figure 23 reveal the complex history of the faulty weld much more clearly than the peak variance method discussed earlier in this paper. Put simply, it can be seen that the weld goes from ’stable – unsatisfactory’ to ’satisfactory’ to ’unstable – unsatisfactory’, which is an accurate description of the situation.

Figures 21–23 make it clear that this polynomial comparison – which could be easily incorporated into a computer based, on line monitoring system, has the capacity to identify process anomalies even in complex situations. The authors recommend that this avenue be investigated by future developers of laser processing monitoring equipment.

5. Conclusions

Kalman filtering is a superior method to cut-off filtering for extracting data from noisy signals.

Signal variance data can be used in conjunction with raw signal data to improve the sensitivity and robustness of laser welding monitoring devices.

Reflected pulse shape comparisons involving polynomial best fits are a very promising tool for on-line process monitoring for pulsed laser welding.

Acknowledgments

The authors are grateful to VINNOVA – The Swedish Innovation Agency (project DATLAS, no. 2006-00668) and to Laser Nova AB, Östersund, Sweden for their funding and cooperation in the research.

References

[1] www.precitec.com

[2] www.prometec.com

[3] Tonshoff H K, Ostendorf A and Specker W, "Online monitoring and closed-loop control of laser welding processes," vol. 1405. *In Proc. of 12th Int. Symp. for Electromachining (ISEM)*, May 1998, pp. 603–612.

[4] Kaierle S, Beersiek S, "Online control of penetration depth in laser beam welding," vol. 3. Aachen, Germany: Industrial Electronics Society, 1998. IECON '98. *Proc. of the 24th Ann. Conf. of the IEEE*, Sep 1998, pp. 1694–1698.

[5] Norman P, Engström H, Kaplan A. F. H: State-of-the-art of monitoring and imaging of laser welding defects, *Proc. NOLAMP 11, August 20-22, 2007, Lappeenranta (FIN),* Ed.: V. Kujanpää (2007).

[6] Gustafsson F, *Adaptive Filtering and Change Detection*, Wiley, New York (2000).

[7] http://www.cs.unc.edu/~welch/kalman/

[8] Greval M, Andrews A, *Kalman Filtering Theory and Practice using MatLab*, J. Wiley 2001, ISBN 0-471-39254-5

[9] Kalman, R. E (1960). A New Approach to Linear Filtering and Prediction Problems.
Transaction of the ASME—*Journal of Basic Engineering*, 82(Series D), 35-45.

Appendix 1. Kalman filtering

The Kalman filter is named after R.E. Kalman who, in 1960, presented a paper [9] describing a recursive solution to the problem of discrete data linear filtering of a time varying process with measurements disturbed by noise.

The Kalman filter is an algorithm rather than an actual filter. Mathematically it is the optimal solution for the linear-quadratic problem i.e. estimating a systems "state" whether it may be observable or not using measurement data and minimizing the quadratic error of estimation error covariance.

The filter has found a widespread use from telecommunication to image processing, control theory and military applications such as target tracking etc. A good introduction to the subject can be found in [7] and a more thorough derivation in [6]. MatLab applications are treated in [8].

The observed reflection signal $y(t)$ in our experiment was modelled as a sum of the reflection signal $s(t)$ (reflected laser light) plus white noise $n(t)$ with covariance R. I.e. the received signal can be written as

$$y(t) = s(t) + n(t) \tag{1}$$

The received signal was modelled in discrete time as an nth order Auto Regressive (AR)-process [6] i.e.:

$$y_k = a_1 y_{k-1} + a_2 y_{k-2} +++ a_n y_{k-n-1} \tag{2}$$

plus a piecewise linear trend between consecutive samples represented at time instant k as b_1+b2_k. When combining these two into one we can write the received signal y_k as:

$$y_k = a_1 y_{k-1} + a_2 y_{k-2} ++ a_n y_{k-n-1} + b_1 + b_2 k =$$

$$\begin{bmatrix} y_{k-1} & y_{k-2} & \cdot\cdot & y_{k-n-1} & 1 & 0 \end{bmatrix} \begin{bmatrix} a_1 \\ a_2 \\ \cdot\cdot \\ a_{n-1} \\ b_1 \\ b_2 k \end{bmatrix} = CX_k \tag{3}$$

i.e. in matrix formulation: $Y_k = CX_k$ (4)

Using arcov off line in MatLab to estimate the AR coefficients identified that a model order of 2 was sufficient.

I.e. the process can be modelled with two coefficients as a first order degree polynomial

$$y_k = a_1 y_{k-1} + a_2 y_{k-2} \qquad (5)$$

b_1 and b_2 could now be estimated for each iteration and subtracted from the measured values y_k.

Using Kalman formulation we had:

The internal state of the process: X (6)

The state transition matrix A:

$$A = \begin{pmatrix} & & 0 & 0 & 0 \\ I_{nxn} & & \cdot\cdot & \cdot\cdot & 0 \\ 0 & & .. & 1 & 1 \\ 0 & & .. & 0 & 1 \end{pmatrix} \qquad (7)$$

Kalman gain K_k (8)

Covariance of the estimation error: $y_k - \hat{y}_k$ P_k (9)

Covariance of the measurement noise: R (10)

The Kalman equations are given in their iterative form as follows;

$$K_k = AP_k C_k^T \,/\, (C_k P_k C_k^T + R) \qquad (11)$$

$$X_{k+1} = AX_k + K_k (y_k - C_k X_k) \qquad (12)$$

$$P_k = (A - K_k C_k) P_k (A - K_k C_k)^T + K_k R K_k^T \qquad (13)$$

$$\hat{y}_k = C_k X_k \qquad (14)$$

where y_k is the observed (measured value) and $\hat{y}_k$ is the estimated value (used in later calculations).

Appendix 2. The CUSUM algorithm

To detect the leading and trailing edges of the reflected laser light signal the CUmulative SUM (CUSUM) - algorithm has been used. The CUSUM algorithm is defined as follows [6]:

Assume that we want to detect a change in mean of magnitude. ν of the signal $s(k)$

We first form an objective function $g(k)$:

$$g(k) = \max(g(k-1) + s(k) - \nu, 0); \text{alarm if } g(k) > h \tag{15}$$

where the alarm level h is a design parameter and ν is an offset .To detect negative changes we simply use min instead and negate both h and ν. If we now use $\hat{y}_k$ as $s(k)$ then , when the alarm is triggered, the actual reflection value $\hat{y}_k$ $\hat{y}_k$ is picked from the most probable time of change into $peak(k)$. As a rule of thumb [6] the value is taken at the point

$$k - h/(0.5 - \upsilon) \tag{16}$$

i.e.

$$peak(k) = \hat{y}(k - h/(0.5 - \upsilon)) \tag{17}$$

and remains constant until the next peak is detected.

For every sample instant k, the variance $\operatorname{var}(k)$ was calculated in a straight forward manner as:

$$\operatorname{var}(k) = \tfrac{1}{5} \sum_{j=k-5}^{k} (peak(j) - m)^2; k = 6..N. \tag{18}$$

(Note that $peak(k)$ is a vector of length N but piecewise constant between each peak)

N is the number of samples and *m* the overall mean of the peaks, i.e. the average peak value. The number 6 was chosen as a compromise the get a reasonably fast response.

In a real world application it would of course be possible to use e.g. an electronic trigger signal from the laser to identify the rising edge of the signal and e.g. a leaky capacitor solution to detect the peak. An advantage of using CUSUM is that this algorithm is robust to noise and gives a statistically significant indication of an actual change in the measured signal.

Paper III

Challenges to the Interpretation of the Electromagnetic Feedback from Laser Welding

Challenges to the Interpretation of the Electromagnetic Feedback from Laser Welding

R. Olsson[1,2], I. Eriksson[1], J. Powell[1], A. V. Langtry[3] and A.F.H. Kaplan[1]

[1] Luleå University of Technology, SE-971 87 Luleå, Sweden;
www.ltu.se/tfm/produktion
[2] Laser Nova AB, SE-831 48 Östersund, Sweden;
[3] GE Healthcare, Oxford, UK.

E-mail: rickard.olsson@lasernova.se; Alexander.kaplan@ltu.se

Abstract

This paper considers the point that it is not possible to interpret individual weld perturbations from the raw electromagnetic feedback collected from laser weld zones. The presentation of electromagnetic data as a 3D cloud is presented as a new, useful tool in the analysis of this feedback. For example, it is shown that there is a very low correlation between the plasma or thermal signals and the reflected light signal from the weld zone, and that a strong correlation exists between the plasma and thermal signals. It is also demonstrated that data points from a weld perturbation form a different 3D cluster to those from the stable welding process. A strategy for future on line data analysis is presented in the use of a suitably shaped data cloud envelope. The rates of data fit to the various segments of such an envelope could be correlated with specific weld anomalies.

Introduction

The practice of industrial laser welding often involves continuous monitoring in order to optimise productivity. A common feedback technique involves the use of photodiodes to

monitor the electromagnetic emissions from the weld zone. These emissions can be divided into three wavelength ranges associated with reflected laser light, thermal radiation from the weld zone and the higher temperature radiation from the plasma or gas cloud above the weld. Figure 1 describes the optical arrangement of sensors which have individual sensitivities to reflected light (R), thermal radiation (T) and plasma radiation (P).

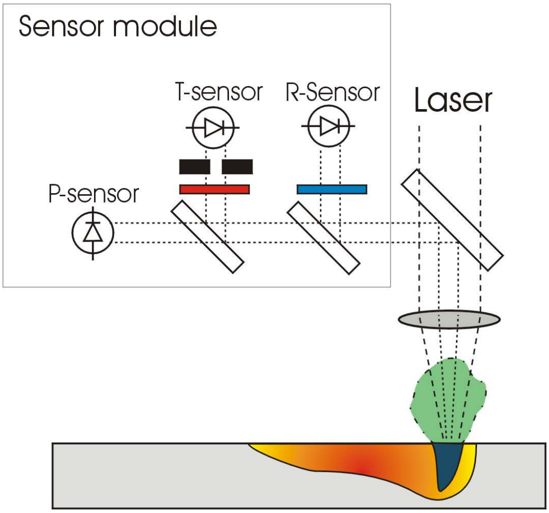

Figure 1. The arrangement of the Reflected light (R), Thermal radiation (T) and Plasma radiation (P) sensors, which monitor the electromagnetic radiation from the laser welding process.

The signals generated by the photodiodes are continuously compared to a "golden template" of signals historically associated with good quality welds for the specific application involved. Excessive deviation from the 'good weld' signal envelope triggers an alarm, which may be used to halt the welding process.

This type of monitoring has been developed by purely empirical means with minimal theoretical back-up [1,2]. The work presented in this paper forms part of the early stages of a full analysis of this method of weld monitoring. The eventual outcome of this branch of research should be an improved understanding of the correlation between the signals generated within the weld zone and the defects produced in the welds.

The three sensor configuration shown in figure 1 is an adaptation of an original two sensor set-up used to monitor welding carried out with CO_2 lasers. The original CO_2 laser welding monitors employed only a thermal (infra-red) sensor sensitive over the range of wavelengths from 1300nm to 1800nm and a plasma (ultra-violet) sensor, sensitive to wavelengths below 600nm. The UV range of the plasma sensor is particularly appropriate for CO_2 laser welding because the metal vapour boiling off from the weld zone absorbs a substantial proportion of the incident laser light and becomes heated to an ionised plasma state. The stability and intensity of the UV light generated by this plasma can be indicator of weld quality during CO_2 laser welding.

During Nd:YAG welding the plume of vapour above the weld zone is transparent to the laser beam and does not become heated to a plasma state. This hot vapour radiates as a black body radiator, emitting light over a continuous spectrum

Welding of Zn-coated steel is also well known for its instability and proneness for blow outs due to excessive gas pressure. Welding of Zn-coated steel has been thoroughly investigated by e.g. Norman et.al.[3], Fabbro et.al. [4] and Heyden et.al. [5].
A thorough survey on the state of the art of process monitoring of laser welding can be found in [6].
The reflected light sensor involves a photodiode with a behind a narrow bandpass filter around the laser wavelength and the level of reflected light detected is dependant on the weld pool geometry. Often this R-sensor signal will have a higher variance for bad welds then for good welds because an unstable welding process leads to an extremely variable weld pool surface.

Fig 2 is a schematic graph of the observed wavelengths and the light emitted during Nd:YAG welding.

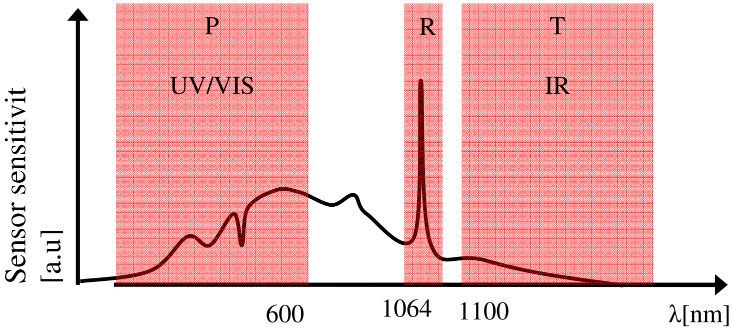

Figure 2 A schematic of the wavebands of the three monitoring sensors (Plasma, Reflected and Thermal).

Statistical signal processing work has been carried out by a number of workers including Fennander et.al. [7], who looked at Laser hybrid welding using data from high speed imaging fed to a Kalman filter for droplet tracking in conjunction with Principal Component Analysis (PCA) and vector machines for the classification of data. In this case the PCA was used to interpret and simplify the time based 2D-data from the cameras.

A similar approach was also used by Jäger [8], who introduced the concept of "Eigen –meltpools". i.e. mutually orthogonal surface shapes corresponding to the first four eigenvalues–eigenvectors for a typical welding situation. Jäger et al also describe both the advantages and drawbacks involved in using Independent Component Analysis (ICA) [9] for surface classification. One of their findings was that ICA showed no significant improvement over PCA and their conclusion was therefore that second order statistics (e.g. PCA) are sufficient for surface description and classification.

For conventional arc welding Mirapeix et al. [10] used PCA to interpret spectral data from the weld pool temperature signal. The PCA components were later fed to a trained Artificial Neural Net (ANN) for defect classification. In their work they showed that the following defects could be detected using this technique;

- slight lack of penetration
- lack of penetration
- low welding current
- inert gas flow reduction

Experimental work and discussion

In this paper we used the commercial monitoring system Weldwatcher from Precitec, and synchronised the measurements to a high speed camera (Photron SA1).

The experimental setup used was:

- Material: 2 x 0.8 mm thick zinc coated steel.
- Laser source: 3kW Haas 3006L Lamp pumped Nd:YAG
- Power 2.5kW CW
- Optics: 600um step index fibre with 250 mm collimator and f=200mm
- Feed rate: 5m/min.

Two welds were produced under the same processing conditions but the fit up geometry of the welds were different – as shown in figure 3. It is well know that, when laser lap welding zinc coated steel, the best results are usually achieved if a clear path is provided for the escape of the zinc vapour boiling off the surfaces of the sheets which are in contact [3,4,5]. In the welds produced for this experiment, this clear path was provided in one case (as shown in figure 3a), but the other weld involved close contact between the sheets and no escape route for the vapour. This latter arrangement had the expected consequence of a liquid eruption or ‘blow out’ of the weld. Both welds were approximately 180mm long and took 2 seconds to complete. The welds will be identified throughout the rest of this paper as the ‘good’ weld and the ‘blow out weld’. The sampling rate of the sensors was 20 kHz and the blow out took place approximately halfway through the weld and lasted approximately 1.5ms. This paper will compare the data from both welds, concentrating on the differences caused by the blowouts.

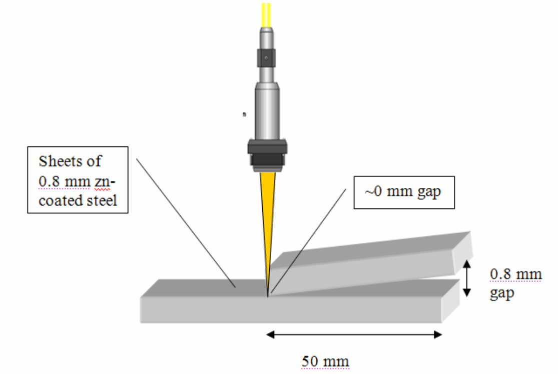
Sheets of 0.8 mm zn-coated steel
~0 mm gap
0.8 mm gap
50 mm

Fig 3a Experimental situation for the good weld

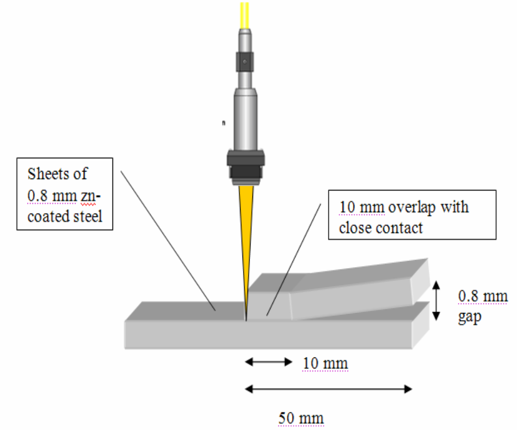
Sheets of 0.8 mm zn-coated steel
10 mm overlap with close contact
0.8 mm gap
10 mm
50 mm

Fig 3b Experimental situation for the blow out weld

Figure 4 presents the raw data from the three sensors for the good weld and the blow out weld. There appears to be a close correlation between the temperature and plasma signals in both cases. It is also clear that the signals are less stable in the case of the blow out weld although there is a considerable level of noise in both sets of signals.

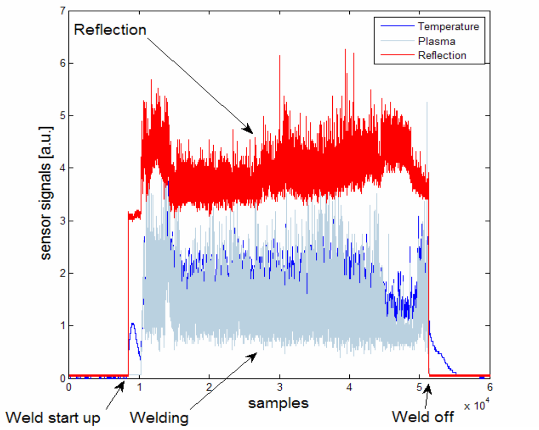

Figure 4a.

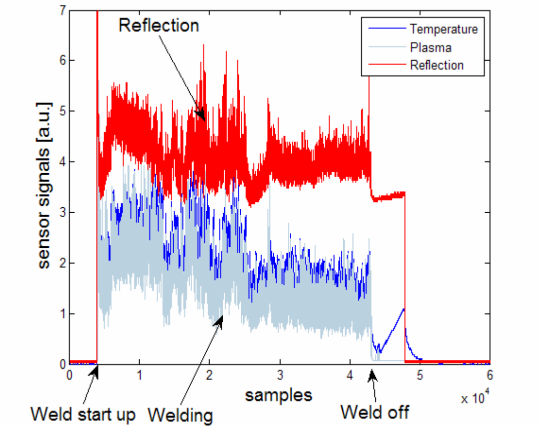

Figure 4b.

Figure 4. Raw data from the three sensors for; a.The good weld and b.The blow out weld.

It is, of course, very difficult to interpret the data if it is presented in its raw form – although data readings of this type can be used in conjunction with simple threshold values. Extra information can be gathered from the data if it is presented as a three dimensional cloud – as in figure 4. In this case the three data points from every individual time instant are presented as a single point inside a three dimensional graph. For example, if, sometime during the first second of welding, we take our 15,024th reading of the T, R and P signals – the values might be 2.4, 1.2 and 4.5 respectively. We then plot the point 2.4, 1.2, 4.5 on our x,y,z graph – the time element of the information is hidden in this type of display, but we can see the general correlation of the whole data set. In figure 5 we can see that there is some correlation between the data points whilst the welding is taking place – and we can also see that the start up and ending phases of the welding process produce sets of data points which are clearly separate from the main cloud. The welding process is, in effect, disrupted during the start up and ending phases and these 'disturbed' welding periods provide distinct, coherent groups of data points. This means that it might be possible to identify specific weld perturbations such as blow outs (see figure 6) or keyhole collapse, by their data point signatures in the three dimensional space of such a graph. Even at this early stage of these results it is interesting to note that the data signature start up phase of the blow out weld is completely different from, and far less cohesive than, that of the good weld – indicating an inherent instability as a result of vapour pressure building up beneath the weld pool.

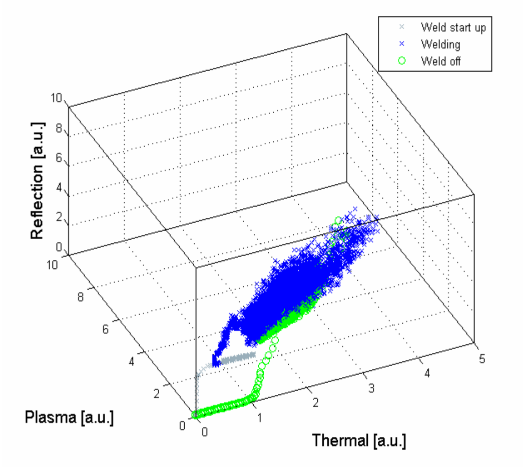

Figure 5a. Good weld

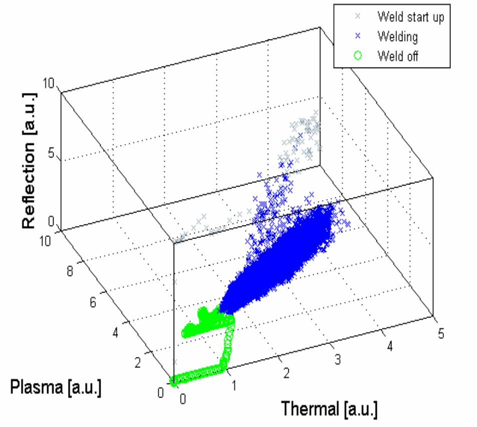

Figure 5b. Blow out weld

Figure 5 shows data clouds taken from the information presented in figure 4.

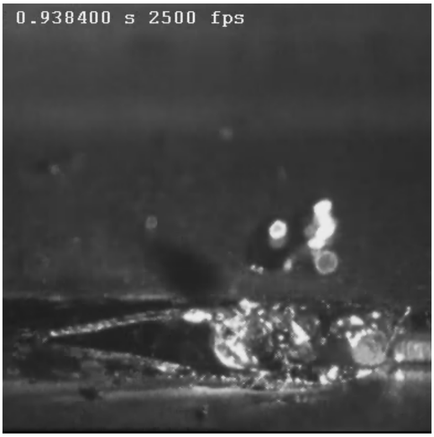

Figure 6. A weld experiencing a 'blow out' – trapped zinc vapour blows a hole in the weld pool as it escapes - leading to the ejection of a considerable amount of liquid.

Although the differences between the start up and ending phases of the weld are interesting, we are really working towards an on line monitor of the main part of the welding process. Figure 7 presents the data clouds of figure 4 with the start up and ending phases removed.

In these figures the overall mean has been subtracted from all the data values to generate a zero mean data cloud. This is to enable correct PCA calculations for the resulting eigenvectors shown in subsequent figures.

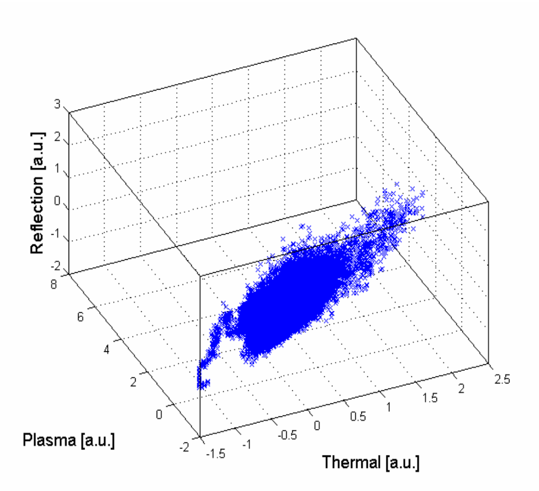

Figure 7a.

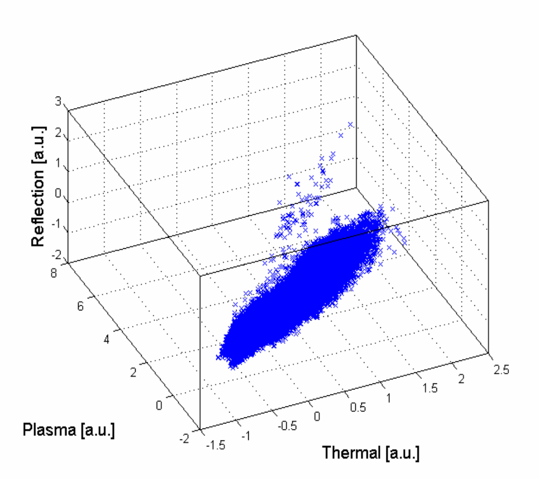

Figure 7b.

Figure 7. The good weld (7a) and blow out weld (7b) data clouds after the start and end phases of the welding process have been removed. In these figures the overall mean has been subtracted from all the data values to generate a zero mean data cloud.

Figure 7 reveals that there are clear similarities and differences between the two data clouds. The overall cloud shapes and their orientations in the 3D space are similar – but there are considerably more outlying points in the case of the unstable weld.

If we look at the overall shape and orientation of the clouds first, we can extract some information from the three side views of the 3D data field – as shown in figures 8,9 and 10.

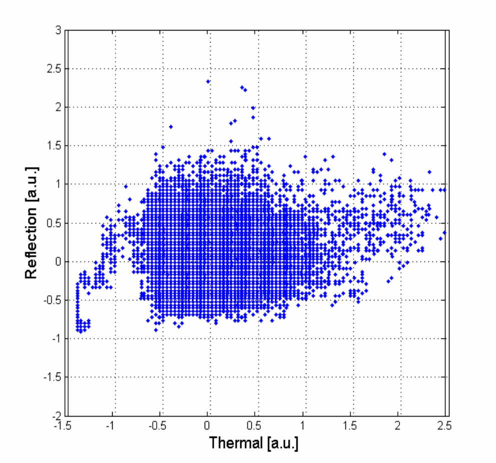

Figure 8a.

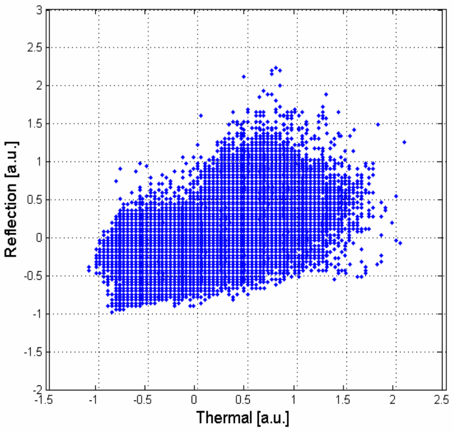

Figure 8b.

Figure 8. The reflection/temperature relationship of the data clouds for a. the stable and b. the unstable welds.

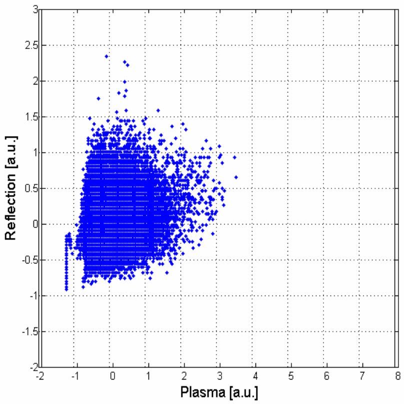

Figure 9a.

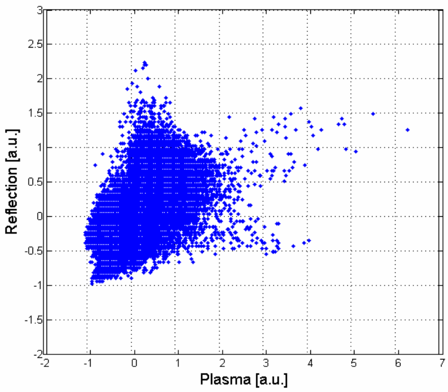

Figure 9b.

Figure 9. The reflection/plasma relationship of the data clouds for a. the good and b. the blow out welds.

Figures 7 and 9 reveal that there is a very low correlation between the plasma or thermal signals and the reflected light signal. This low correlation can be explained by the fact that the strength of the reflected signal from the weld zone will largely be dependant on the surface geometry of the melt rather than the temperature of the melt or the vapour cloud.

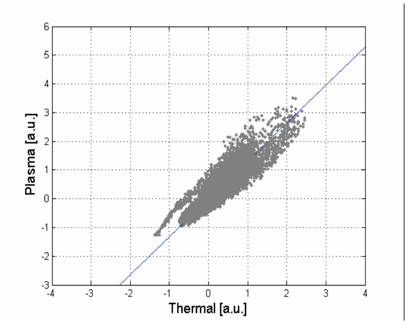

Figure 10a.

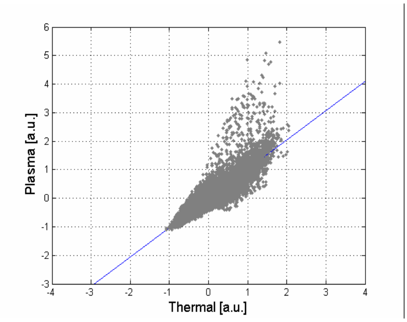

Figure 10b.

Figure 10. The plasma/temperature relationship of the data clouds for a. the good and b. the blow out welds.

Figure 10 shows that there is a strong correlation between the plasma and thermal signals from the weld zone. This strong correlation could be expected because the rate of vapour generation is governed by the weld pool temperature. Increased weld pool heating will result in increased boiling and so the two thermal signals are linked.

Picking the largest eigenvalues and corresponding eigenvectors from the PCA analysis of the data clouds we can identify the direction vector pointing in the direction of maximum variation $dirVect$ for the good weld as:

$$dirVect = \begin{bmatrix} 0.60 \\ 0.79 \end{bmatrix} \quad (in \begin{bmatrix} Thermal \\ Plasma \end{bmatrix} direction) \tag{1}$$

and for the blow out weld as:

$$dirVect = \begin{bmatrix} 0.65 \\ 0.67 \end{bmatrix} \quad (in \begin{bmatrix} Thermal \\ Plasma \end{bmatrix} direction) \tag{2}$$

Much of difference between the coefficients can be attributed to the “tail” seen in figs 7a, 8a and 9a which affects the principal component vector. Otherwise it is clear that the core 3D geometry of the clouds for both welds is similar.

We can now consider the detailed shape of the blow out weld data in a search for a correlation between weld perturbations and specific data clusters in the 3D cloud. Although the time-based information relevant to each data point is not displayed in the data cloud, it is possible to identify each point from the basic data set. Using the time base given by the high speed video film, it is therefore possible to label the points in the data cloud which are associated with the blow out – these are presented in figure 11 as light points.

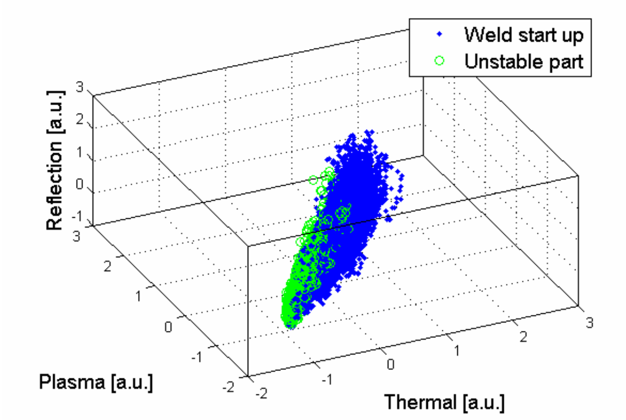

Figure 11 the data cloud for the blow out weld with the data points associated with the blow out identified as light points and the stable periods of this weld identified by the dark points.

From the process monitoring point of view, it is encouraging that the data points for the blow out event are not evenly spaced within the data cloud – there is a clear tendency for them to cluster in one sector of the overall cloud. The blow out data is associated with a quadrant of the 3D space where all three signal levels are low but the plasma signal is larger than average for the thermal and reflected signals involved. This could be related to the increased vapour evolution during blow out. The zinc vapour will join the iron vapour – the level of which may also be increased as a result of increased melt surface area – because the weld zone is much more undulating than normal and airborne droplets are present in the area. The low reflection signal associated with blow outs is also traceable to a physical phenomenon. The reflectivity of the weld decreases with increased melt surface curvature, because a flat weld would be the most effective reflector of the laser light, and the weld surface is considerably more curved when blow outs are taking place. In order to investigate the various shapes of the data clouds for the ‘stable’ and ‘blow out’ parts of the weld, the two are presented separately in figures 12 and 13.

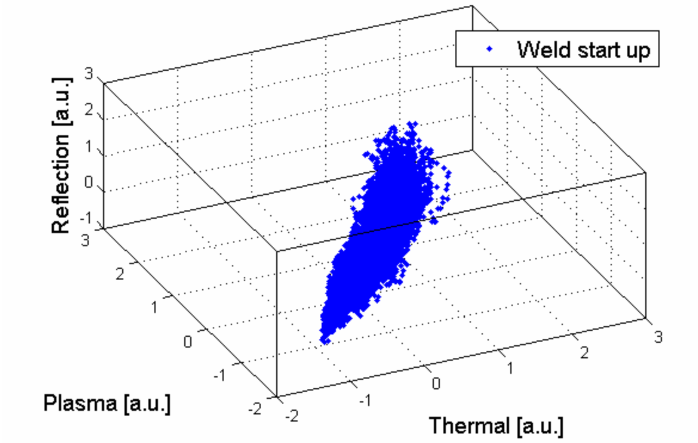

Figure 12. The data cloud from figure 11 with the ’blow out’ data removed. This is the shape of the data cloud for the stable part of this weld.

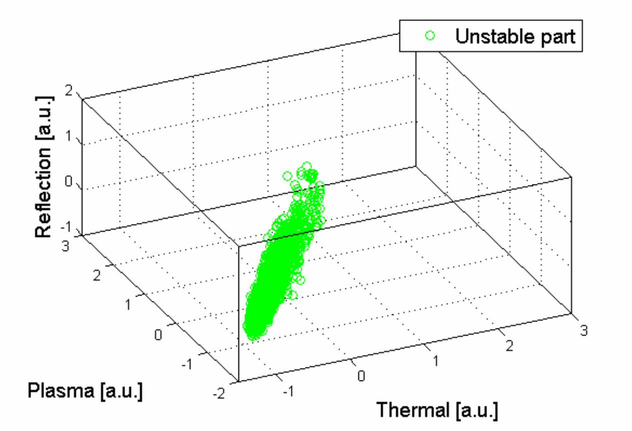

Figure 13. The data cloud for the ‘blow out data only.

Figures 13 and 14 demonstrate that the two sets of data both form coherent clouds, but give no indication of the overlap between the two. To assess the level of overlap, figure 14 presents two cross sectional slices of the data cloud taken across the ‘thermal’ axis. When the 3D space is rotated so that we view it from the end with the plasma/reflection axes, as in figure 15, we can see the intermingling of the ‘blow out’ and ‘stable welding’ data points. From the images in figure 15, two things are clear; a. the relative proportions of ‘blow out’ and ‘stable weld’ data points change as we move down the long axis of the data cloud, and b. the distribution of the ‘blow out’ data points is not uniform across the cloud cross section (for example, the upper left quadrant of the larger cross section contains relatively few ‘blow out’ data points).

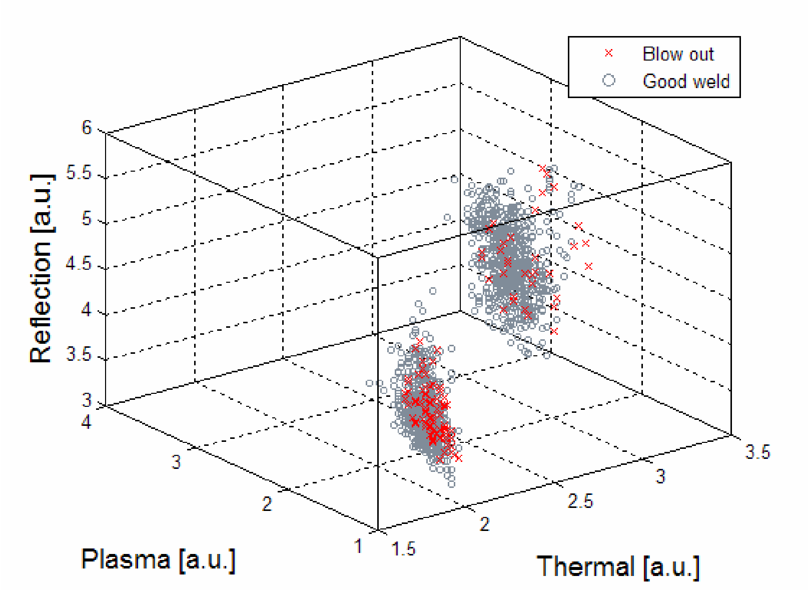

Figure 14. Taking two cross-sections of the data cloud.

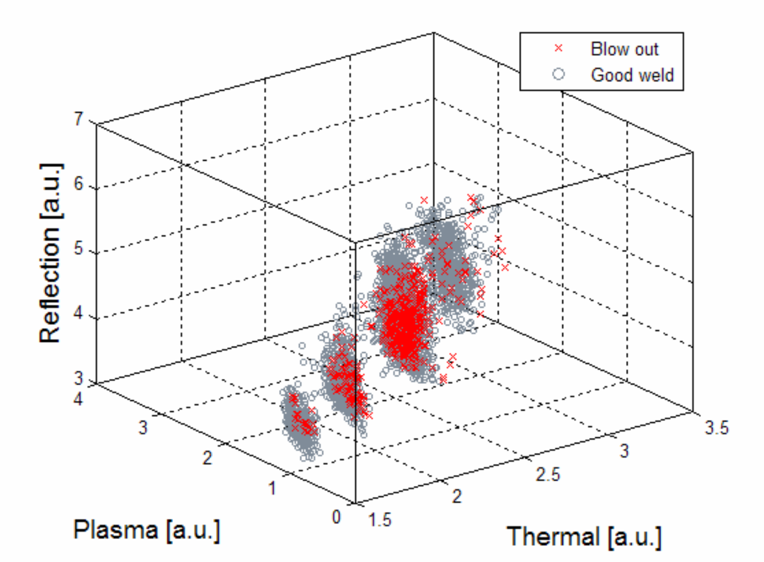

Figure 15. Four cross-sections of the data cloud.

The asymmetric distribution of the blow out data point cloud within the stable weld cloud presents us with a possible future strategy for feedback analysis. This would involve the construction of a suitably dimensioned ellipsoid shell divided into eight segments – as described in figure 16. As data points are acquired from the process they could be converted to their 3D format and would fill the various quadrants of the shell. The relative rates of arrival of the data points into the segments would be an indicator of the state of the welding process and could be compared to the rates for a stable weld. Additionally, the extension of the segments outside the shell to the limits of the 3D 'box' could give another clearly defined eight zones for data collection and rate comparison. This principle will be the subject of future work by the present authors.

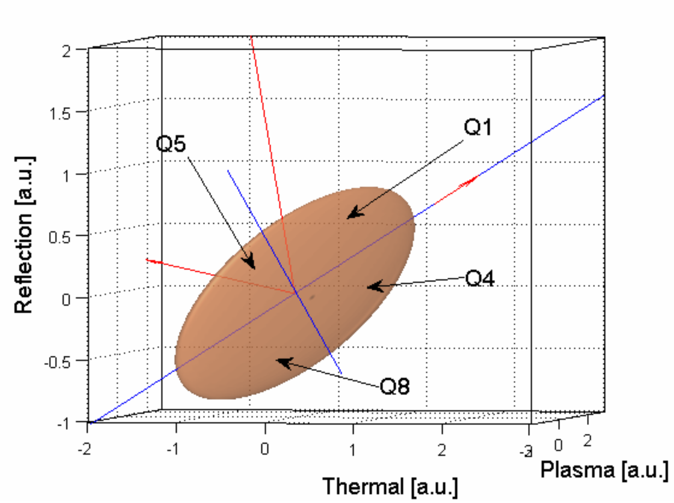

Figure 16. A strategy for on line data analysis could involve a standard cloud divided into eight or more sectors.

Conclusions

- It is not possible to interpret individual weld perturbations from the raw electromagnetic data collected from laser weld zones.
- The presentation of electromagnetic data as a 3D cloud provides a new, useful tool in the analysis of feedback from laser weld zones.
- There is a very low correlation between the plasma or thermal signals and the reflected light signal from the weld zone.
- There is a strong correlation between the plasma and thermal signals from the weld zone.
- Data points from a weld perturbation (blow out) form a different 3D cluster to those from the stable welding process.

- A strategy for future on line data analysis is the use of a suitable data cloud envelope or multi-layered envelopes. The rates of data fit to the various segments of such envelopes could be correlated with specific weld anomalies.

Acknowledgments

The authors are grateful to VINNOVA – The Swedish Innovation Agency (project DATLAS, no. 2006-00668) and to Laser Nova AB, Östersund, Sweden for their funding and cooperation in the research.

References

[1] www.precitec.com

[2] www.prometec.com

[3] P. Norman, I. Eriksson, A. F. H. Kaplan Monitoring Laser beam welding of zinccoated sheet metal to analyze the defects occurring, Proc. 12th NOLAMP, August 24-26, 2009, Copenhagen (DK), FORCE Technology

[4] R. Fabbro, F. Coste, D. Goebels and M. Kielwasser, 2006. Study of CW Nd-Yag laser,Welding of Zn-coated steel sheets. Journal of Physics D: Applied Physics, 39(2), pp. 401-409.

[5] J. Heyden, K. Nilsson, C. Magnusson ,Laser Welding of Zinc Coated Steel, Lasers In Manufacturing, Jun., 1989, p. 161-167

[6] P. Norman, H. Engström, A. F. H. Kaplan: State-of-the-art of monitoring and imaging of laser welding defects, NOLAMP 11, August 20-22, 2007, Lappeenranta (FIN), Ed.: V. Kujanpää (2007).

[7] H. Fennander, V. Kyrki, A. Fellman, A. Salminen, and H. Kälviäinen. Visual measurement and tracking in laser hybrid welding. *Mach. Vision Appl.*, 20(2):103–118, 2009.

[8] M. Jäger ; F. A. Hamprecht. Principal component imagery for the quality monitoring of dynamic laser welding processes. *Industrial Electronics, IEEE Transactions on*, 56(4):1307–1313, April 2009.

[9] E. Oja, A. Hyvarinen and J. Karhunen,. *Independent Component Analysis*. Wiley-Interscience, May 2001.

[10] J. Mirapeix, P.B. García-Allende, A. Cobo, O.M. Conde, J.M. López-Higuera. Real-time arc-welding defect detection and classification with principal component analysis and artificial neural networks. *NDT and E International*, 40(4):315–323, 2007.

.

Paper IV

Ripple formation on the surface of laser spot welds

Ripple formation on the surface of laser spot welds

I Eriksson[1], R Olsson[1,2], J Powell[1], A F H Kaplan[1] and O Sundelin[2]

[1]Luleå University of Technology, SE-971 87 Luleå, Sweden
[2]Lasernova AB, Odenskogsvägen 1, 831 48 Östersund, Sweden

Email: ingemar.eriksson@ltu.se

Abstract

During laser spot welding of titanium surface ripples were found to originate from melt pool oscillations. The combination of oscillation in the melt pool and a fast solidification froze the oscillations as ripples on the surface. The solution to the problem was to delay the solidification until the oscillations were dampened out. By pulse shaping, ripple free weld spots were created.

1. Introduction

Microscopic examination of laser spot welds frequently reveals surface ripples such as those shown in figure 1. Ripples of this sort could be unacceptable in some production environments because of their effect on the fatigue life or the visual appearance of the weld.

Both numerical simulation and experimental research has shown oscillation [1, 2] of the melt pool during laser welding. High speed imaging of laser-induced wave formation in a liquid Sn- or Zn-pool [3] illustrates these oscillations in the absence of a solid-liquid boundary redirecting the flow. Numerical simulation of the resolidification process during spot welding [4,5] has provided an understanding of the cooling behaviour with respect to time, particularly its dependence of pulse duration and beam radius. Computation of the recoil pressure from laser-induced evaporation during initiation of keyhole laser welding [1,6] has modelled the melt pool flow, particularly the radial acceleration of the melt perpendicular to the solid-liquid interface. In pulsed Nd:YAG spot welding ripples have been found to originate from the oscillations [1,2] of the weld pool. When the weld pool solidifies fast [4,5] the oscillations are frozen to become ripples on the surface.

Note that the present phenomenon takes place in a certain power density window high enough to achieve the boiling point but at interaction times which are too low to allow keyhole drilling.

This paper describes an experimental program which investigates the process of the ripple formation and suggests a strategy to minimise the effect. The phenomenology of ripple formation has been examined by high speed photography under high intensity illumination and the strategy for ripple minimisation involves suitable power modulation of the laser pulse.

2. Experimental set-up

The experiment involved pulsed Nd:YAG welding of titanium. The Laser used was a ROFIN-SINAR P500. The laser pulse was 1,5 ms long with a repetition rate of 5Hz and 30% of the available peak power (3 J/pulse). The welded part was moved between pulses to produce a weld seam. The feed rate was adjusted to give 50% overlap of the pulses. The shielding gas employed was Argon. To observe the welding a Redlake X3 high speed camera at 8000 frames per second was used with and a Cavilux illumination laser at a power of 500 Watts. Figure 2 is a magnified view of the finished weld considered in this experimental program, showing the overlap geometry and the surface ripples on the individual spot welds.

3. Results and Discussion

Examination of high speed filming shows that the oscillation frequency of the melt pool is approximately 3kHz and the time from turning off the laser to completely solid surface is 3ms.

3.1 High speed photography of ripple formation.

Figure 3a-g presents a series of still photographs from high speed filming of the creation of a single pulse spot weld.

From this series of photographs it can be inferred that the progression of events which results in a set of concentric ripples on a single pulse spot weld is as follows;

The laser pulse starts its interaction with the material and begins to melt the surface.

The weld pool grows in volume and diameter as the laser continues to irradiate the surface. A depression forms in the middle of the weld pool as a result of localised boiling – which exerts a pressure on the melt.

The laser pulse ends and boiling ceases. Surface tension forces the melt to attempt to spring back from a concave geometry to a convex one.

The momentum of the melt in the direction perpendicular to its surface makes the melt surface overshoot its equilibrium position. The melt surface assumes damped simple harmonic motion around its equilibrium position, and this generates surface ripples.

The melt solidifies before this action has died down and the ripples are frozen into the surface topology of the weld.

3.2 Pulse shape modulation to suppress ripple formation.

A series of experiments was carried out to establish the most effective pulse shape to minimise ripples in the eventual weld topology. The overall strategy was to extend the molten life of the melt so that the ripples could die away before solidification took place. Productivity was not affected by this technique because the original pulse frequency of 5Hz was maintained – the post weld heating was accommodated in the gap between the pulses. The original 1.5ms rectangular power profile of the pulse was extended at a lower power level as shown in figure 4. Successful welds with minimum surface rippling were produced at an extended pulse lifetime of 4ms, and an increase of pulse power to 7 J/pulse

Figure 5 demonstrates that the majority of the surface ripple effect has been suppressed although there is some evidence of minor rippling at the edge of the solidified melt where cooling and solidification rates are at their highest.

4. Conclusions

In the latter stages of the laser-melt interaction during pulsed laser spot welding, the central portion of the weld is depressed as a result of localised boiling which exerts a pressure on the melt. As the laser pulse ends, the boiling ceases, and the pressure is removed. The melt then begins to return to its equilibrium geometry under the influence of surface tension, but the vertical momentum of the melt carries it past this equilibrium position. The surface then experiences damped simple harmonic motion. Ripples on the surface of the solid welds are created by rapid solidification of a surface which was undergoing damped simple harmonic motion. By delaying the solidification until the harmonic motion is completely dampened, surface ripples can be avoided.

Acknowledgements

The authors are grateful to VINNOVA – The Swedish Innovation Agency (project DATLAS, no. 2006-00668) for funding the project, and to Lasernova AB for supporting the research.

References

[1] Cho J,Farson D, Milewski J and Hollis K 2009 Weld pool flows during initial stages of keyhole formation in laser welding *Journal of Physics D-Applied Physics* **42** 175502

[2] Klein T, Vicanek M and Simon G 1995 Forced oscillations of the keyhole in penetration laser beam welding *Journal of Physics D-Applied Physics* **29** 322-332

[3] Mizutani M, Katayama S and Matsunawa A 2002 Observation of molten metal behavior during laser irradiation - Basic experiment to understand laser welding phenomena *Proc SPIE* **4831** 208-13

[4] He X, Elmer J W and DebRoy T 2005 Heat transfer and fluid flow in laser microwelding *Journal of applied physics* **97** 84909

[5] He X, Fuerschbach P W and DebRoy T 2003 Heat transfer and fluid flow during laser spot welding of 304 stainless steel *Journal of Physics D-Applied Physics* **36** 1388-1398

[6] Semak V V, Knorovsky G A, MacCallum D O and Allen Roach R 2006 Effect of surface tension on melt pool dynamics during laser pulse interaction *Journal of Physics D-Applied Physics* **39** 590–5

Figures

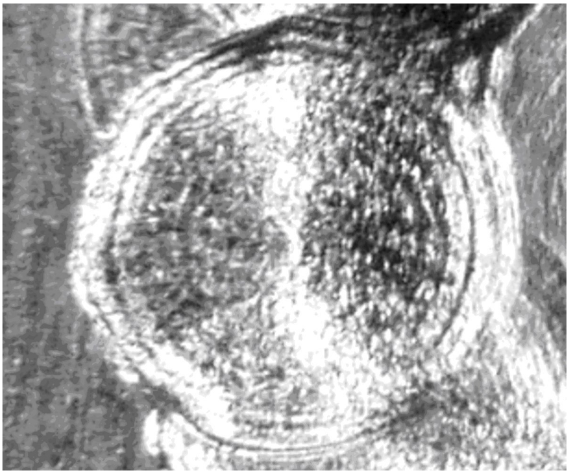

Figure 1. The rippled topography of typical pulsed laser weld in titanium.

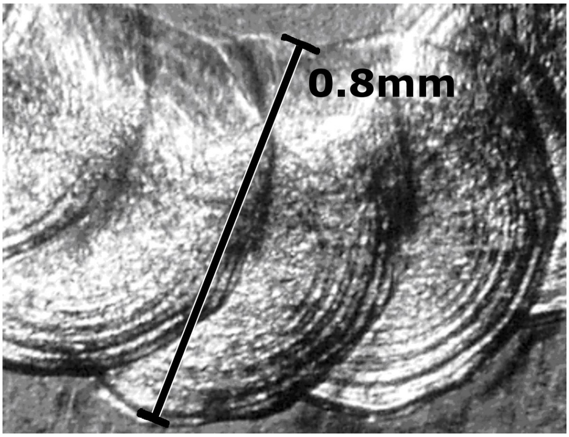

Figure 2. The overlap geometry of the spot welds investigated.

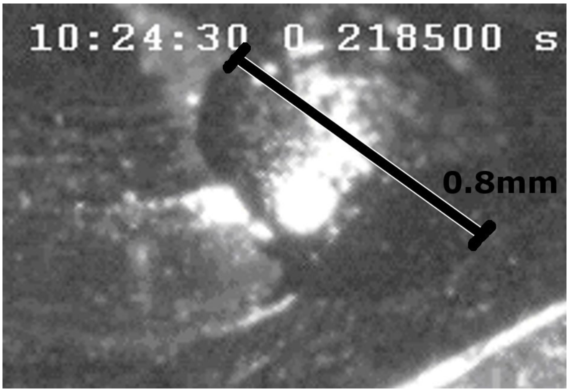
10:24:30 0.218500 s
0.8mm

Figure 3a Here we see the previous, solidified spot weld

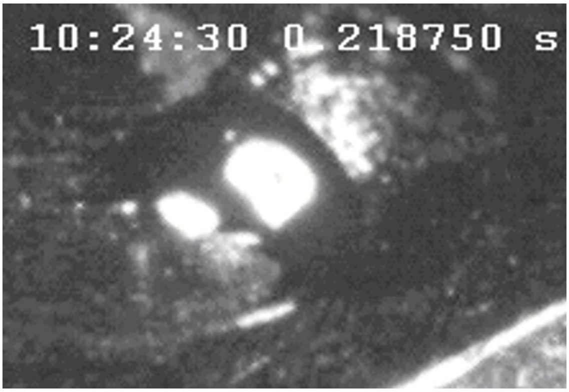
10:24:30 0.218750 s

Figure 3b As the pulse irradiates the position of the next spot weld the material begins to melt.

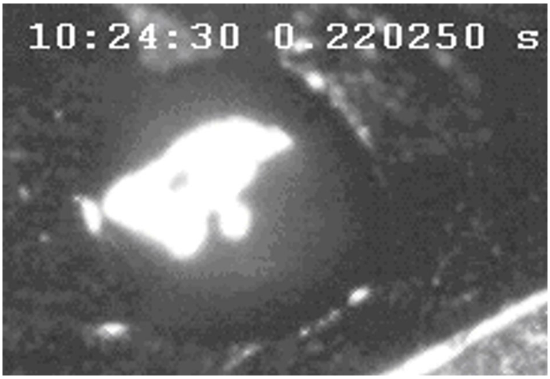
10:24:30 0.220250 s

Figure 3c Melting continues and is eventually accompanied by boiling. The recoil pressure of the boiling action causes the top of the melt to become flattened or dimpled. And the melt is pushed laterally away from the centre [5].

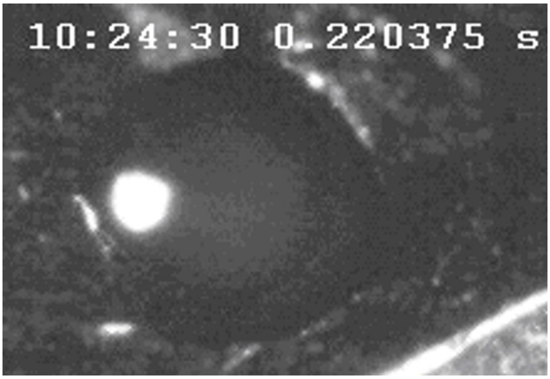

Figure 3d As the laser pulse ends, boiling ceases and the melt tries to assume a hemispherical geometry under the influence of surface tension.

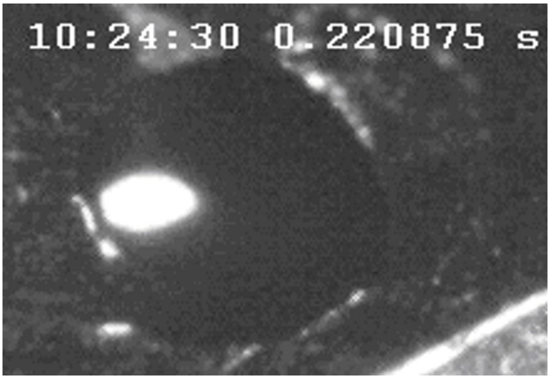

Figure 3e The sudden upward movement of the melt surface initiates damped simple harmonic motion. This motion can be seen as the glare of the illumination changes shape.

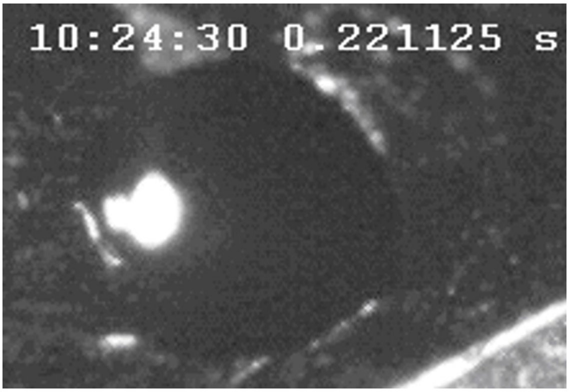

Figure 3f The melt pool solidifies from its base upwards and from the edges inwards, too quickly for the ripples to die away.

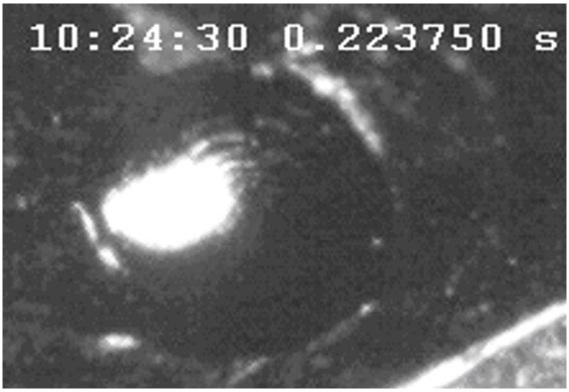

Figure 3g The ripples are frozen in place on the surface of the weld.

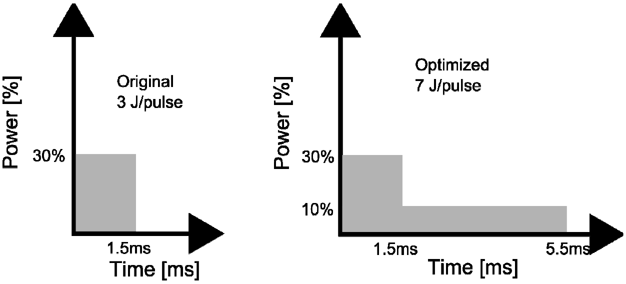

Figure 4. Pulse shaping minimizes the ripples

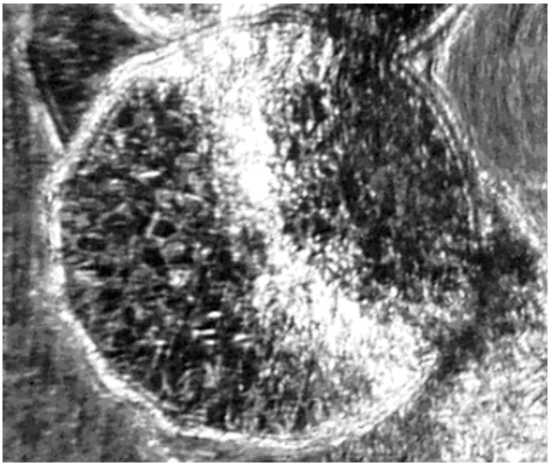

Figure 5. Pulse with less ripples